

## **Hydrodynamical simulations in FLUENT**

Carl Erik Wasberg and Bjørn Anders Pettersson Reif

Norwegian Defence Research Establishment (FFI)

19th April 2010

FFI-rapport 2010/00930

113701

P: ISBN 978-82-464-1752-3

E: ISBN 978-82-464-1753-0

## Keywords

Fluiddynamikk - Numeriske metoder

Hydrodynamikk

Vingeprofiler

## Approved by

Bjørn Anders Pettersson Reif

Project Manager

Jan Ivar Botnan

Director

## English summary

A methodology for hydrodynamical simulations in FLUENT is described. The current application is the computational fluid dynamics analyses of two- and three-dimensional wings conducted as part of an underwater towing project (reported in Ø. Andreassen et al.: "*Hydrodynamic design and analysis of tail fish*", FFI-report 2010/00136), but the methodology is applicable to more general hydrodynamical problems.

The Navier-Stokes equations for incompressible viscous fluid flow are solved using the software package FLUENT. The main results from these simulations are lift, drag, and moment coefficients of the wings, as a function of angle of attack. Grid design and the application of a turbulence model are discussed in the report.

Two-dimensional wing profiles with available reference data for air flow are used to verify the simulations. Then the same profiles are simulated in water, together with some alternative profiles. Finally, two different three-dimensional delta wings are simulated in water. It is shown that the size of the computational domain has a strong influence on the drag coefficients in two dimensions, but much less in three dimensions.

The results obtained in this work have been used in the underwater towing project.

## Sammendrag

Denne rapporten beskriver en metodikk for hydrodynamiske simuleringer i FLUENT. Den aktuelle anvendelsen er fluiddynamikk-simuleringer av to- og tredimensjonale vinger utført som en del av et undervanns-taueprosjekt (beskrevet i Ø. Andreassen et al.: "*Hydrodynamic design and analysis of tail fish*", FFI-report 2010/00136), men metodikken er anvendbar for mer generelle hydrodynamiske problemer.

Navier-Stokes-ligningene for inkompressibel viskøs strømming er løst med simulering-programmet FLUENT. Hovedresultatene fra disse simuleringene er koeffisienter for løft, drag og moment for vingene, som funksjon av angrepsvinkel. Design av grid og anvendelse av en turbulensmodell er diskutert i rapporten.

Todimensjonale vingeprofilene med tilgjengelige referansedata i luft er brukt til å verifisere simuleringene. Deretter er de samme profilene simulert i vann, sammen med noen alternative profiler. Til slutt er to forskjellige tredimensjonale deltavinger simulert i vann. Det vises at størrelsen på beregningsområdet innvirker sterkt på drag-koeffisientene i to dimensjoner, men mye mindre i tre dimensjoner.

Resultatene fra dette arbeidet har blitt brukt i undervanns-taueprosjektet.

# Contents

<b>1</b>	<b>Introduction</b>	<b>7</b>
<b>2</b>	<b>Methodology</b>	<b>7</b>
2.1	Computational domains and grids	8
2.2	Using the Spalart-Allmaras model in FLUENT	10
2.3	Two-dimensional simulations: The NACA-0009 airfoil	11
2.4	Two-dimensional simulations: The NACA-65209 airfoil	15
<b>3</b>	<b>Other two-dimensional simulations</b>	<b>17</b>
3.1	The E-817 wing profile	17
3.2	The SF-01 wing profile	19
<b>4</b>	<b>Simulations of three-dimensional hydrofoils</b>	<b>21</b>
4.1	The SF-01-3D delta wing	23
4.2	The E-837-3D delta wing	28
<b>5</b>	<b>Conclusions and recommendations</b>	<b>30</b>
	<b>Appendix A FLUENT reports</b>	<b>33</b>
A.1	FLUENT input report for NACA-0009 in air	33
A.2	FLUENT input report for SF-01 in water	36
A.3	FLUENT input report for SF-01-3D in water	39



# 1 Introduction

The success of hydrodynamical simulations relies on a relevant mathematical model of the physics, correct application of suitable boundary conditions, good design of the computational domain and the computational grid, and an accurate numerical solver. This report describes a methodology for hydrodynamical simulations around rigid bodies, with flow around two- and three-dimensional wings as the present application.

The methodology, described in section 2, is first tested on two-dimensional NACA profiles operating in air with given reference solutions for verification, and then in water. In section 3, it is also applied to a two-dimensional Eppler profile and a new two-dimensional high-lift profile. In section 4, we present simulations for a three-dimensional delta wing based on the new high-lift profile and for a three-dimensional delta wing based on a symmetric Eppler profile, and the conclusions and methodological recommendations are presented in section 5.

Wing-like structures can be used in towed underwater systems for positioning and maneuvering. For application of the results in that context, see the report [2].

## 2 Methodology

The computational fluid dynamics (CFD) simulations are conducted using the software package FLUENT from ANSYS Inc. The governing equations for the cases considered in this report are the Navier-Stokes equations for incompressible viscous flow, and except for some cases with large angles of attack, a statistically steady solution is found. The lift, drag, and moment coefficients of the foil are then calculated from this steady solution.

Calculations on a computational grid fine enough to resolve all the turbulent scales are usually not possible within the available time limits, so the effects of the small-scale turbulent motion must be modelled. In this report, a Reynolds-Averaged Navier-Stokes (RANS) turbulence model is used to simulate the averaged effect of turbulent advection on the mean flow field. The Spalart-Allmaras turbulence model [5] is used, as it is designed for external flows, i.e. flow around bodies. To reduce the grid dependence of the turbulence model, which can sometimes significantly deteriorate the quality of the prediction, the computational grid is refined close to the foil surface, and also in the wake region.

Structured grids with quadrilateral (in two dimensions) or hexahedral (in three dimensions) cells are used in all the calculations presented here. Some comparisons with unstructured grids with tetrahedral cells are given in three dimensions.

Output from the simulations are coefficients of lift, drag, and moment, defined as follows:

$$C_L = \frac{F_L}{\frac{1}{2}\rho_0 v_0^2 A_0}, \quad C_D = \frac{F_D}{\frac{1}{2}\rho_0 v_0^2 A_0}, \quad C_M = \frac{M}{\frac{1}{2}\rho_0 v_0^2 A_0 c_0},$$

where  $F_L$ ,  $F_D$ , and  $M$  are the lift force, drag force, and moment, respectively, acting on the body, and the following reference quantities appear:

- $\rho_0$ : Reference density ( $\text{kg}/\text{m}^3$ ),
- $v_0$ : Reference velocity ( $\text{m}/\text{s}$ ),
- $A_0$ : Reference area ( $\text{m}^2$ ),
- $c_0$ : Reference length (chord length) ( $\text{m}$ ).

It should be noted that the forces acting on the foil can be decomposed into pressure- and frictional forces.

The Reynolds number is defined using the reference velocity and reference length:  $Re = v_0 c_0 / \nu$ , where  $\nu$  ( $\text{m}^2/\text{s}$ ) is the kinematic viscosity.

The coordinate system used for the two-dimensional simulations is shown in figure 2.3, and for the three-dimensional simulations in 4.3. The pitching moment axis is defined as the vector  $[0, 0, -1]$ , with centre in  $(0.25, 0)$  for the two-dimensional foils (25% of the chord length from the leading edge), while the moment centre is given in the text for each of the three-dimensional cases.

The momentum equation is discretized by a second order method in FLUENT. First order discretization is also available, but is only recommended at the start of an iterative solution procedure if there are initial convergence problems. It is illustrated in section 4.1 that the drag coefficients are over-predicted when first order discretization is used. The discretization of the equation for modified turbulent viscosity is not as critical, but second order is preferable here as well.

The boundary conditions are defined as inflow at the left boundary and outflow at the right boundary, while the top and bottom boundaries are periodic. A non-slip boundary condition is applied at the body surface. In three dimensions, an additional symmetry boundary is introduced at the “back” of the computational domain, whereas the free-stream velocity is specified at the “front” boundary.

A summary of FLUENT settings for three of the simulations presented here is given in the Appendix.

## 2.1 Computational domains and grids

Air flow over two-dimensional NACA profiles with available experimental reference solutions are used as test cases to verify the methodology. The NACA-0009 and NACA-65209 are chosen, the former being symmetric and the latter is not. Experimental data for these airfoils are found in [1].

The two-dimensional foils have chord length 1 m and are placed with the leading edge at the origin of the coordinate system. The reference values  $c_0 = 1$  m and  $A_0 = 1$   $\text{m}^2$  are used. Two computational domains are used,  $[-9, 11] \times [-10, 10]$  m (“small”) and  $[-19, 51] \times [-20, 20]$  m (“large”). In the construction of the computational grid, the domains are divided into 22 blocks, as shown for the small domain in figure 2.1. For the large domain, the outer blocks are simply extended to the new



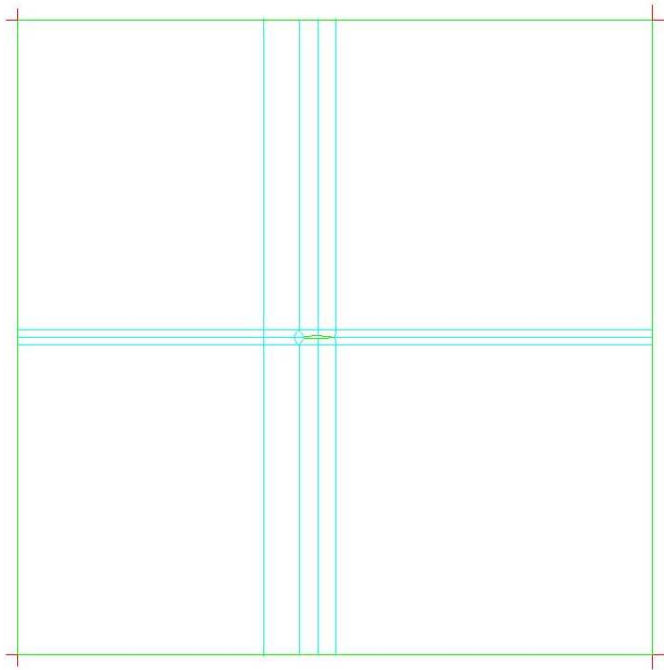


Figure 2.1: The 22 blocks of the small two-dimensional computational domain

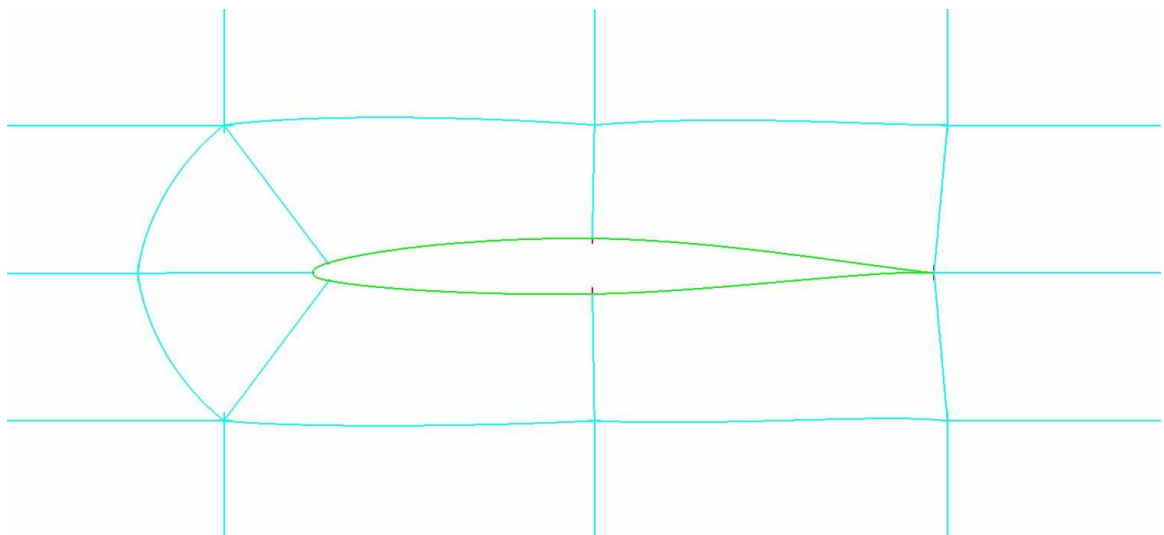


Figure 2.2: Blocking close to a wing profile

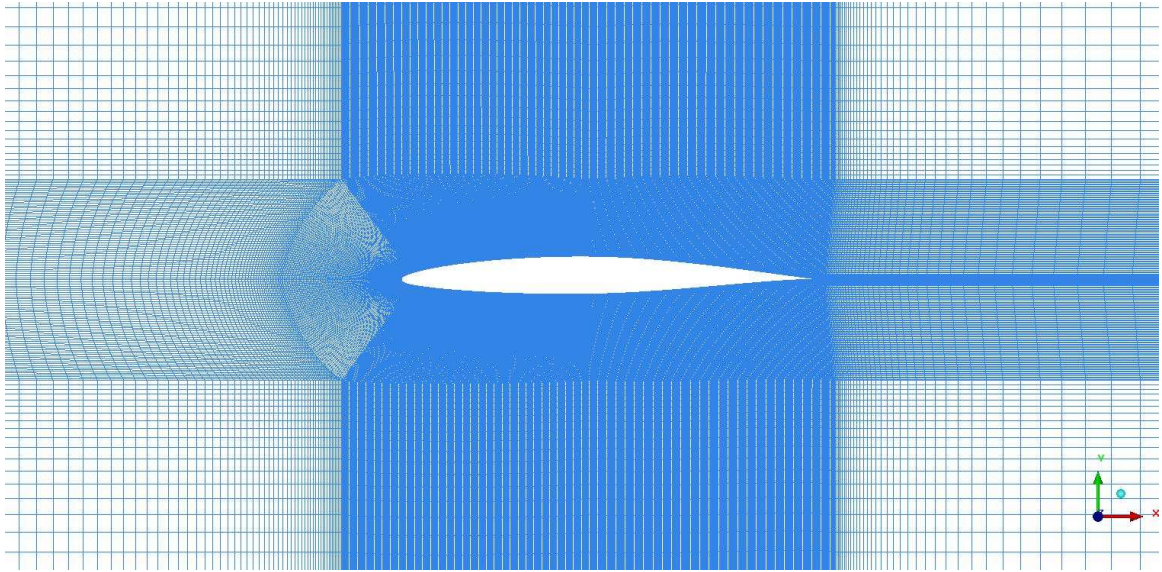


Figure 2.3: Overview of the computational grid around the NACA-65209 airfoil

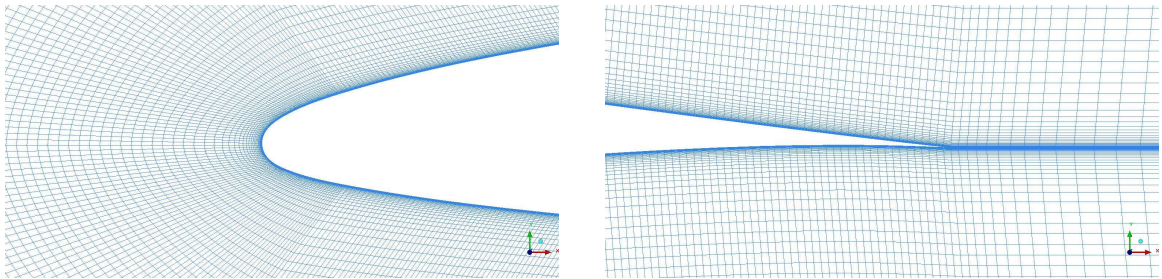


Figure 2.4: The computational grid around the front (left) and back (right) of the NACA-65209 airfoil

domain boundaries. Figure 2.2 shows the blocks close to a wing profile, while the grid around a wing profile is illustrated in figures 2.3 and 2.4. The grids for the small and large domains have 377 thousand and 602 thousand cells, respectively. The grid in the blocks around the body are identical for the two domains, and the thickness of the cells at the body surface is 15–20  $\mu\text{m}$ .

At the Turbulence Modeling Resource web pages from NASA Langley Research Center [4], it is advised that the farfield boundary should be at least 400 chord lengths away from the airfoil to avoid boundary effects on the drag and lift, particularly at high lift conditions. We investigate the effect of the domain size on drag and lift in this report.

## 2.2 Using the Spalart-Allmaras model in FLUENT

The dependent variable in the Spalart-Allmaras model is a modified turbulent (kinematic) viscosity,  $\tilde{\nu}$ , with unit  $\text{m}^2/\text{s}$ . This is identical to the kinematic viscosity,  $\nu$ , except in the near-wall (viscosity-

Inlet boundary condition	$C_L$	$C_D$	$C_M$
$\tilde{\nu} = \nu$ (“TVR = 1”)	0.510	$1.18 \times 10^{-2}$	$-1.19 \times 10^{-3}$
$\tilde{\nu} = 0.001$	0.509	$1.20 \times 10^{-2}$	$-1.30 \times 10^{-3}$

Table 2.1: Lift, drag and moment coefficients for the NACA-0009 airfoil in air, Mach 0.3, angle of attack  $5^\circ$ , for different modified turbulent viscosity values at the inlet boundary

affected) region, where it usually is much larger. The turbulent viscosity is defined as

$$\mu_t = \rho \tilde{\nu} f_{v^1},$$

where

$$f_{v^1} = \frac{\chi^3}{\chi^3 + C_{v^1}^3}, \quad \chi = \tilde{\nu}/\nu,$$

with the constant  $C_{v^1} = 7.1$  [3]. The turbulent viscosity ratio (TVR) is defined as

$$\mu_t/\mu = f_{v^1} \tilde{\nu}/\nu = f_{v^1} \chi = \frac{\chi^4}{\chi^3 + C_{v^1}^3}.$$

It is stated in [4] that the farfield boundary condition for  $\tilde{\nu}$  should be in the range  $3\nu$ – $5\nu$ , which gives TVR in the range 0.21–1.29.

If  $\tilde{\nu} = \nu$ , then  $\chi = 1$ , and the TVR is equal to  $f_{v^1} = 2.79 \times 10^{-3}$ . An apparent inconsistency in FLUENT is that if a TVR of 1 is specified at the inlet, what really happens is that  $\tilde{\nu} = \nu$ , and the TVR becomes  $2.79 \times 10^{-3}$ . However, the default inlet value for modified turbulent viscosity in FLUENT is  $\tilde{\nu} = 0.001 \text{ m}^2/\text{s}$ . For air, this gives  $\chi = 68.5$ ,  $f_{v^1} \approx 1$ , and consequently a TVR of 68.5. The corresponding values for water are  $\chi = 995.2$ ,  $f_{v^1} \approx 1$  again, and a TVR of 995.2. The recommended value for  $\tilde{\nu}$  from [4] lies between these choices.

As shown in table 2.1, the choices  $\tilde{\nu} = \nu_{\text{air}} = 1.46 \times 10^{-5} \text{ m}^2/\text{s}$  and  $\tilde{\nu} = 0.001 \text{ m}^2/\text{s}$  at the inlet boundary give virtually the same calculated lift, drag and moment coefficients. (See also figure 2.7.)

At the outlet boundary, a FLUENT “Outflow” boundary condition was used, in which all the required quantities are extrapolated from the interior. This does not require any specification of turbulent viscosity, as no backflow is assumed.

### 2.3 Two-dimensional simulations: The NACA-0009 airfoil

The NACA-0009 airfoil is shown in figure 2.5. This is a symmetric profile with zero lift in neutral flight and zero pitching moment for small and moderate angles of attack.

The calculated values of  $y^+$  at the first grid point from the wing surface are used as a grid quality check. This is a relevant measure, since the flow is primarily a boundary layer flow.  $y^+$  signifies the non-dimensional distance from the grid point closest to the wall to the wall itself, in relation to the

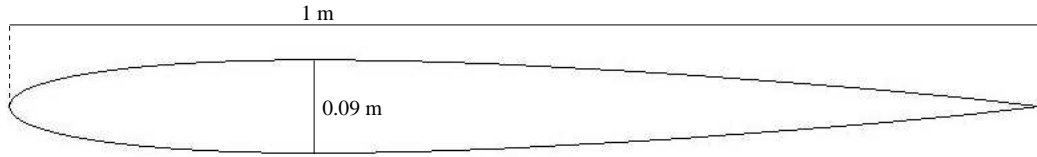


Figure 2.5: The NACA-0009 airfoil

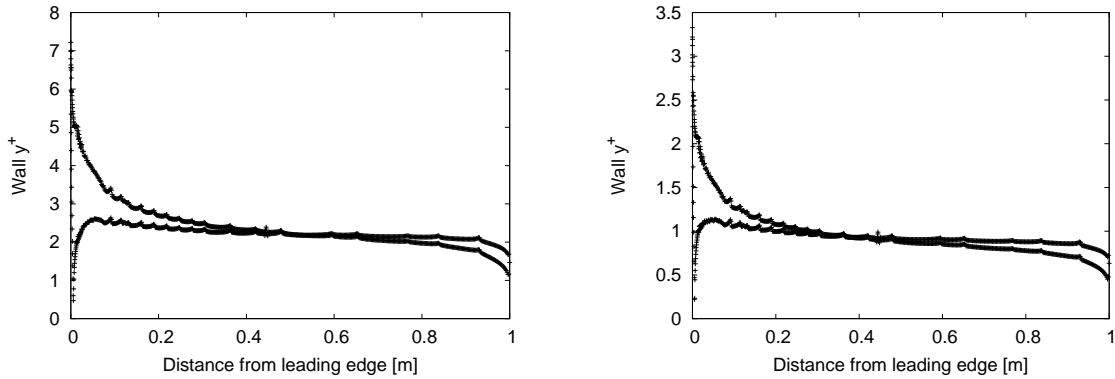


Figure 2.6: Calculated wall  $y^+$  for the NACA-0009 airfoil at  $5^\circ$  angle of attack in air, Mach 0.3, (left) and water, 5 knots (right)

smallest turbulent scale (which becomes smaller with increased Reynolds number  $Re$ ).  $y^+$  is not *a priori* known, but is a function of the solution.  $y^+ = 1$  implies that the distance to the wall equals the smallest turbulent scale. The values for the NACA-0009 airfoil in air and water at  $5^\circ$  angle of attack are shown in figure 2.6. The plots show results from the small domain, but the large domain results are almost identical. The values of  $y^+$  are around 1, so the near-wall resolution is very good.

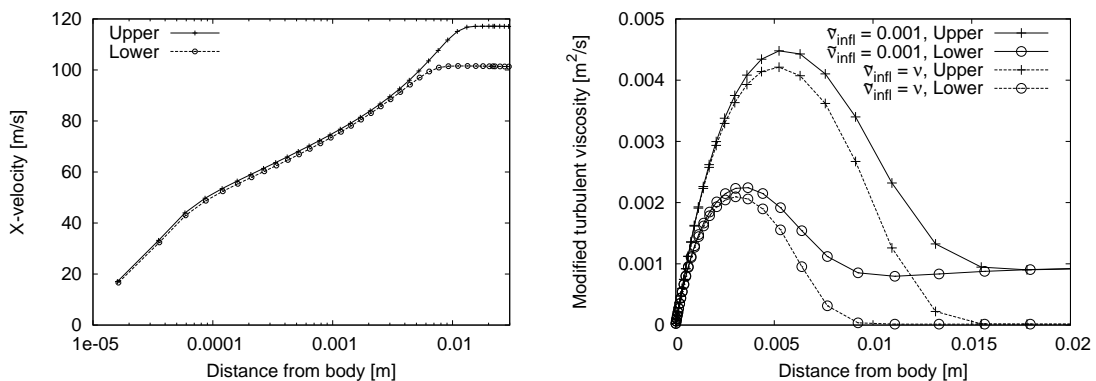


Figure 2.7: Horizontal velocity (left) and modified turbulent viscosity (right) at  $x = 0.5$  for the NACA-0009 airfoil in air (Mach 0.3) at  $5^\circ$  angle of attack

We also check the quality of the grid and the solution by plotting the horizontal velocity component (which is slightly different from the tangential velocity) and the modified turbulent viscosity along

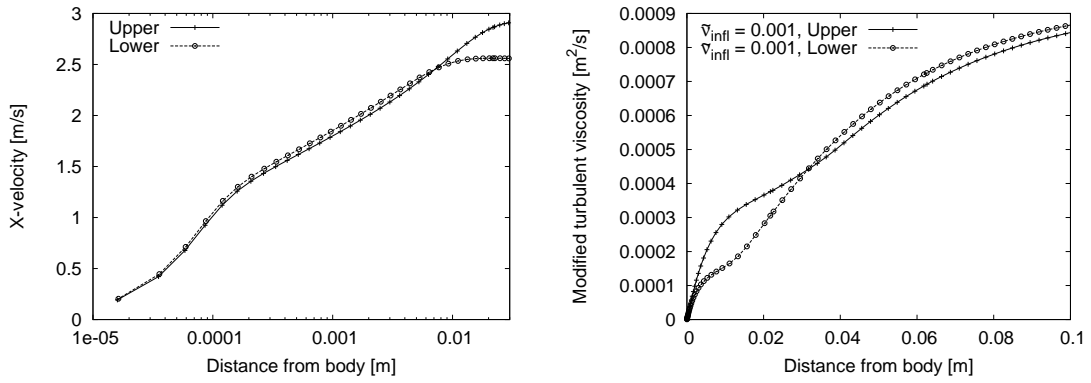


Figure 2.8: Horizontal velocity (left) and modified turbulent viscosity (right) at  $x = 0.5$  for the NACA-0009 airfoil in water (5 knots) at  $5^\circ$  angle of attack

the line  $x = 0.5$ , i.e. through the mid-point of the wing. These results are shown in figures 2.7 and 2.8 for the NACA-0009 airfoil at  $5^\circ$  angle of attack in air and water, respectively. The figures show smooth curves, which indicate that the grid resolution is sufficient around the body.

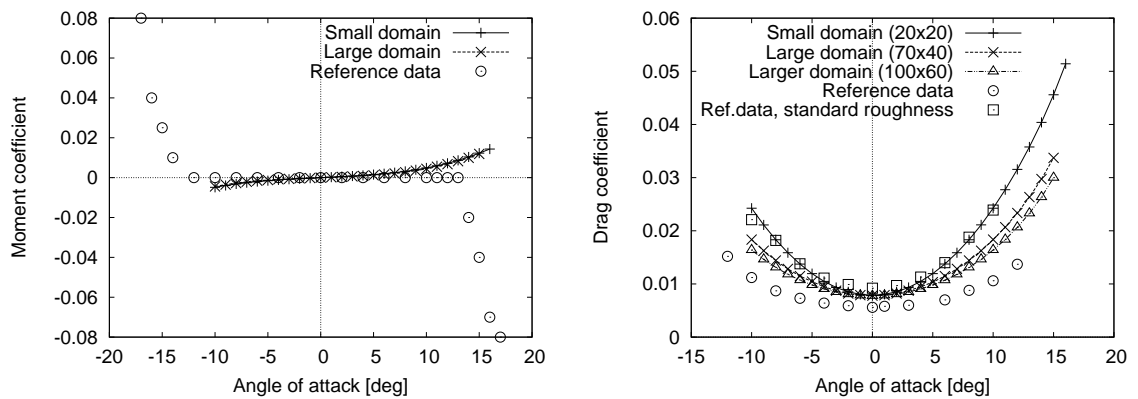


Figure 2.9: NACA-0009 airfoil: Moment (left) and drag (right) coefficients in air, Mach 0.3

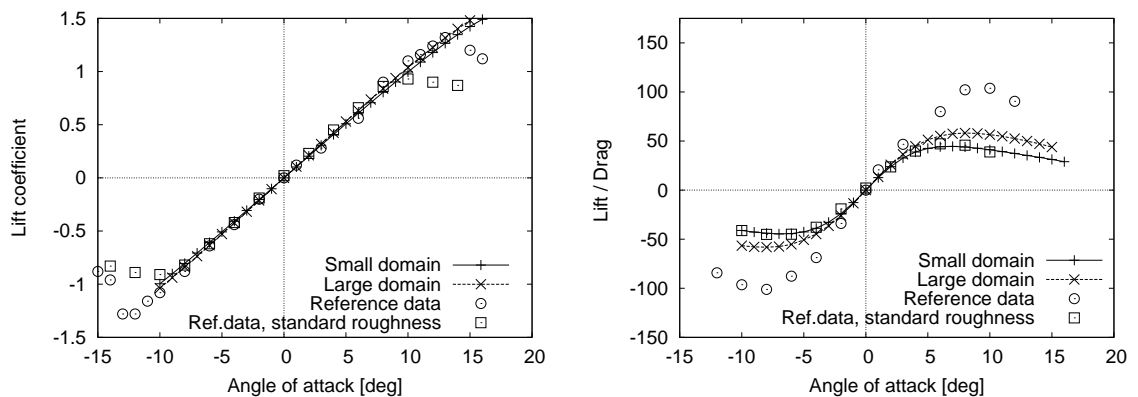


Figure 2.10: NACA-0009 airfoil: Lift coefficient (left) and lift/drag ratio (right) in air, Mach 0.3

Simulations are conducted for Mach 0.3 in air ( $v_0 = 102.9$  m/s,  $Re = 7.04 \times 10^6$ ,  $\rho_0 = 1.225$  kg/m<sup>3</sup>) with angle of attack varying from  $-10^\circ$  to  $15^\circ$ . Coefficients for moment, lift, drag, and lift/drag ratio are given in figures 2.9 and 2.10 and compared with the experimental data from [1]. We observe that the size of the computational domain only influence the drag coefficient, and mainly for absolute values of the angle of attack of  $5^\circ$  and more, where a small domain overpredicts the drag. Simulations for this case were also conducted on an even larger domain,  $[-29,71] \times [-30,30]$  m, and resulted in a further reduction in drag, albeit smaller. If the drag coefficients were critical, further simulations with larger domains would have been necessary. In the context of [2], however, the total drag of the system is dominated by other components, making the present results sufficiently accurate.

Comparison with the experimental data for  $Re = 6 \times 10^6$  (used in the plots here) and  $Re = 9 \times 10^6$  show only minor differences in drag coefficients. These experimental data are obtained using an untripped airfoil, i.e. the boundary layer is not fully turbulent over the wing, but contains a laminar-turbulent transition, which reduces the drag, especially for small and moderate attack angles [4]. It is virtually impossible to simulate such a transition using available models in FLUENT, so it is inherently assumed in the simulations that the boundary layer is fully turbulent everywhere. For application to underwater systems, this is probably also a more realistic scenario. However, data for a “standard roughness” wing at  $Re = 6 \times 10^6$  are also given in [1]. This can be considered a “worst case” roughness for an airplane wing, so it seems reasonable that the calculated drag coefficients lie between the two extremes of untripped and standard roughness data.

The changes in moment and lift characteristics at large positive or negative angles of attack are not captured in the present steady-state calculations, as the experiments indicate stall, whereas the simulations do not. The most likely reason, again, is that the turbulence model overpredicts the turbulence levels on the upper part of the airfoil at large angles of attack. The flow acceleration along the upper surface at high angles of attack “reduces” the turbulence intensity, and this is most likely not captured by the present model.

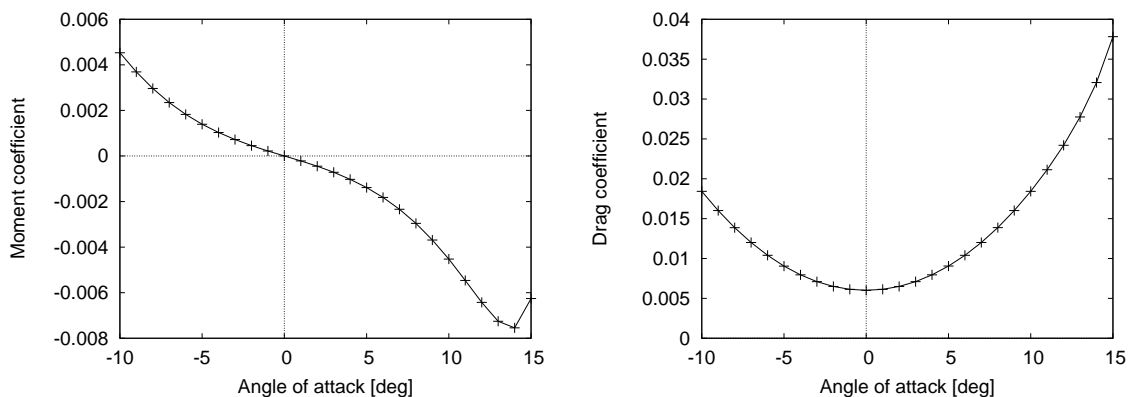


Figure 2.11: NACA-0009 airfoil: Moment (left) and drag (right) coefficients in water, 5 knots

Simulations are also conducted for 5 knots speed in water ( $v_0 = 2.57$  m/s,  $Re = 2.56 \times 10^6$ , Mach



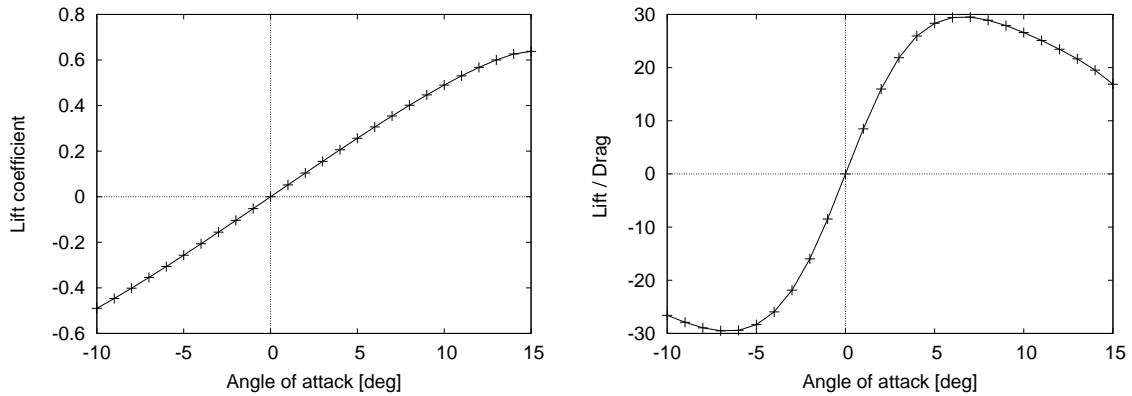


Figure 2.12: NACA-0009 airfoil: Lift coefficient (left) and lift/drag ratio (right) in water, 5 knots

$1.7 \times 10^{-3}$ ,  $\rho_0 = 998.2 \text{ kg/m}^3$ ) with angle of attack varying from  $-10^\circ$  to  $15^\circ$ . Coefficients for moment, lift, drag, and lift/drag ratio are given in figures 2.11 and 2.12. These simulations uses the small domain, so the drag is probably overpredicted. The moment coefficients for the highest angles of attack indicate that there may be problems with these calculations, and unsteady calculations may be needed to capture the flow features. It should be noted that the terminology “unsteady” alludes to a statistically unsteady flow in the present RANS context.

## 2.4 Two-dimensional simulations: The NACA-65209 airfoil

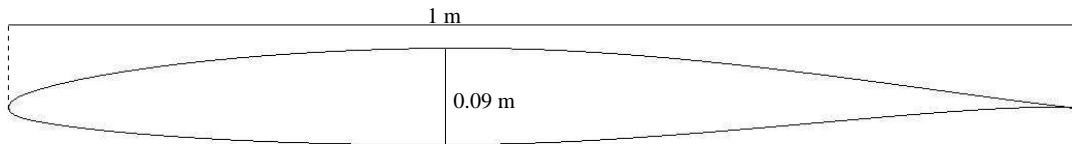


Figure 2.13: The NACA-65209 airfoil

The NACA-65209 airfoil is shown in figure 2.13. This is an asymmetric (or cambered) profile with positive lift in neutral flight, and a negative pitching moment (except for large negative angles of attack, as seen from the reference data in figure 2.14).

Simulations are conducted for Mach 0.3 in air ( $v_0 = 102.9 \text{ m/s}$ ,  $Re = 7.04 \times 10^6$ ,  $\rho_0 = 1.225 \text{ kg/m}^3$ ) with angle of attack varying from  $-10^\circ$  to  $16^\circ$ . Coefficients for moment, lift, drag, and lift/drag ratio are given in figures 2.14 and 2.15, and compared with the reference data from [1]. We observe the same trends as for the NACA-0009 airfoil in the results.

Simulations are also conducted for 5 knots speed in water ( $v_0 = 2.57 \text{ m/s}$ ,  $Re = 2.56 \times 10^6$ , Mach  $1.7 \times 10^{-3}$ ,  $\rho_0 = 998.2 \text{ kg/m}^3$ ) with angle of attack varying from  $-10^\circ$  to  $14^\circ$ . Coefficients for moment, lift, drag, and lift/drag ratio are given in figures 2.16 and 2.17. As for the NACA-0009

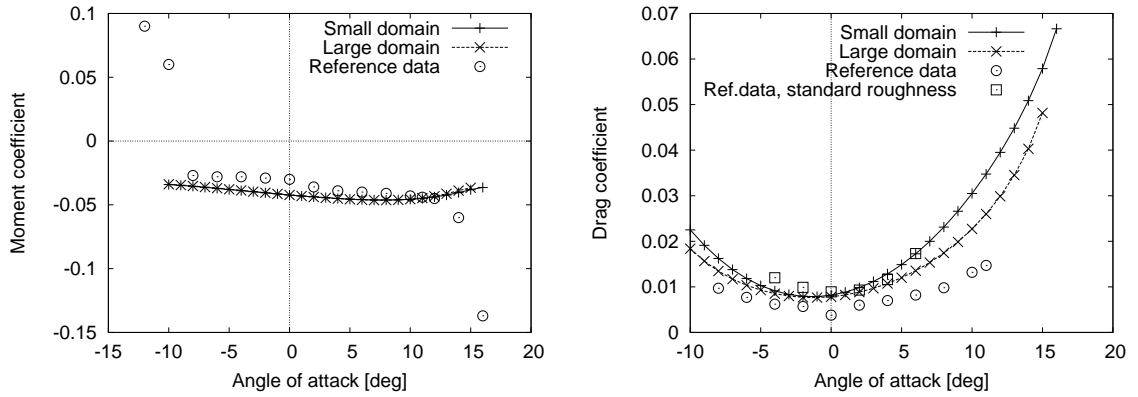


Figure 2.14: NACA-65209 airfoil: Moment (left) and drag (right) coefficients in air, Mach 0.3

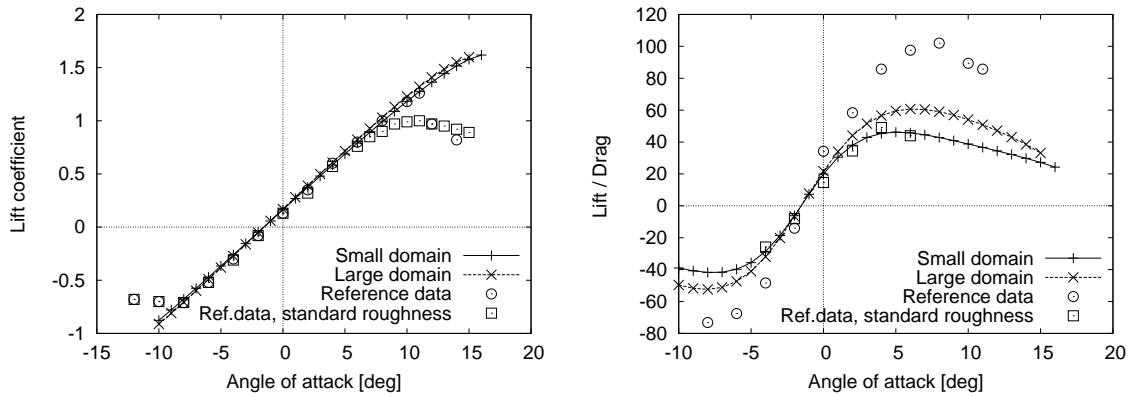


Figure 2.15: NACA-65209 airfoil: Lift coefficient (left) and lift/drag ratio (right) in air, Mach 0.3

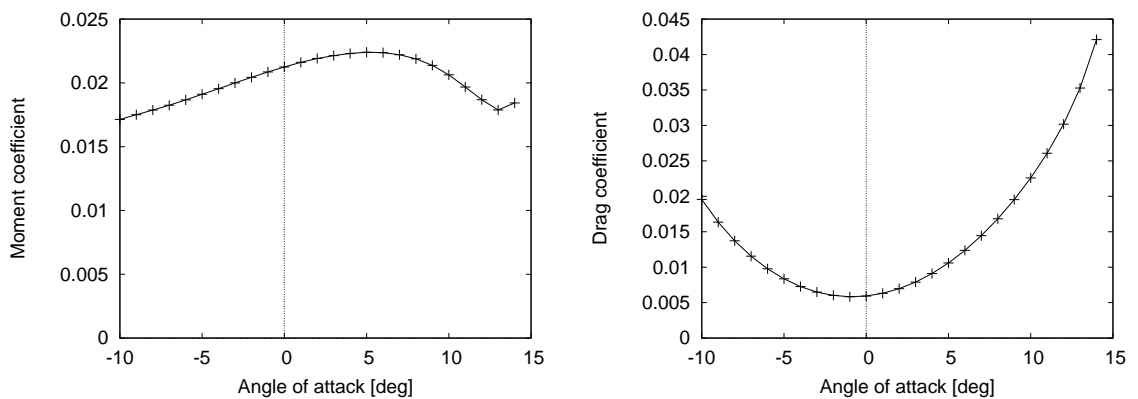


Figure 2.16: NACA-65209 airfoil: Moment (left) and drag (right) coefficients in water, 5 knots



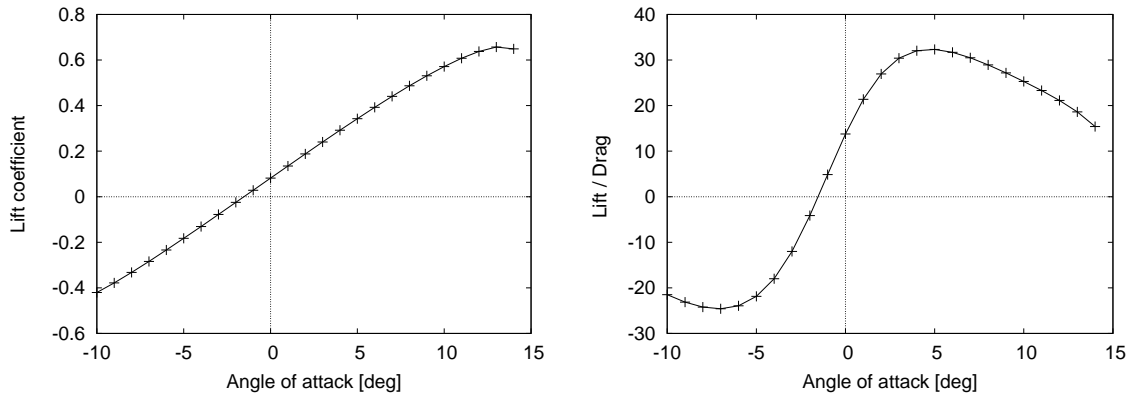


Figure 2.17: NACA-65209 airfoil: Lift coefficient (left) and lift/drag ratio (right) in water, 5 knots

profile in water, the results for the highest angle of attack appear to be less reliable, probably due to stalling and unsteady motion.

### 3 Other two-dimensional simulations

#### 3.1 The E-817 wing profile

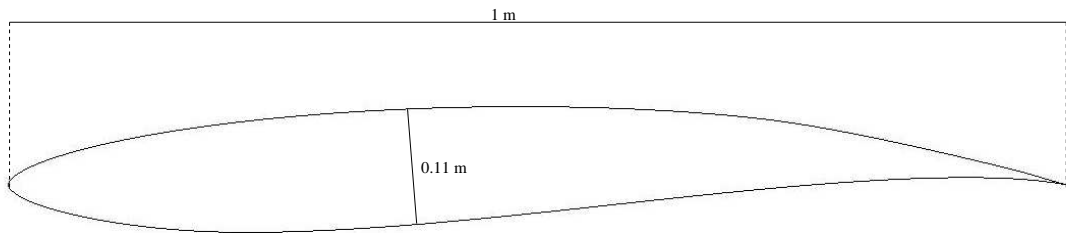


Figure 3.1: The E-817 wing profile

The E-817 (Eppler) wing profile is shown in figure 3.1. This profile is often used in underwater applications. It is included here to compare its performance in water with the NACA-65209 profile.

Simulations are conducted for 5 knots speed in water ( $v_0 = 2.57$  m/s,  $Re = 2.56 \times 10^6$ , Mach  $1.7 \times 10^{-3}$ ,  $\rho_0 = 998.2$  kg/m<sup>3</sup>) with angle of attack varying from  $-10^\circ$  to  $15^\circ$ . Coefficients for moment, lift, drag, and lift/drag ratio are given in figures 3.2 and 3.3. The drag is probably overpredicted, as the small domain is used.

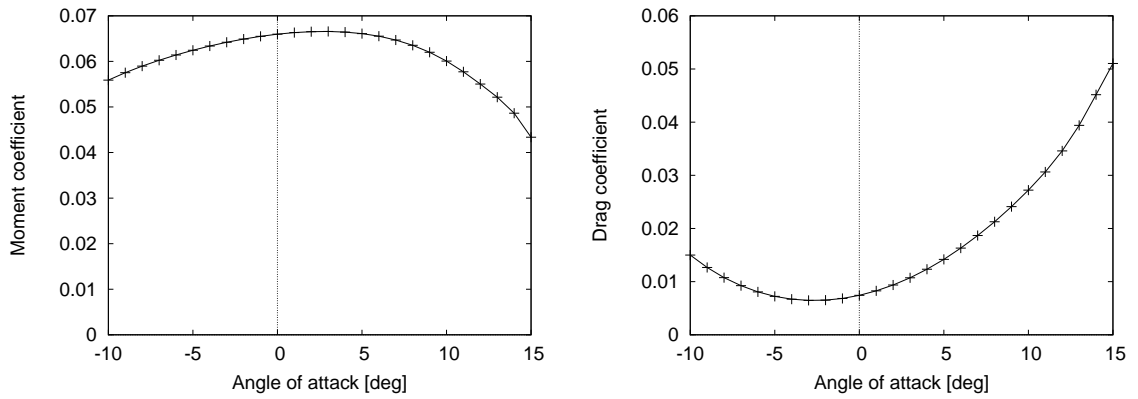


Figure 3.2: E-817 wing profile: Moment (left) and drag (right) coefficients in water, 5 knots

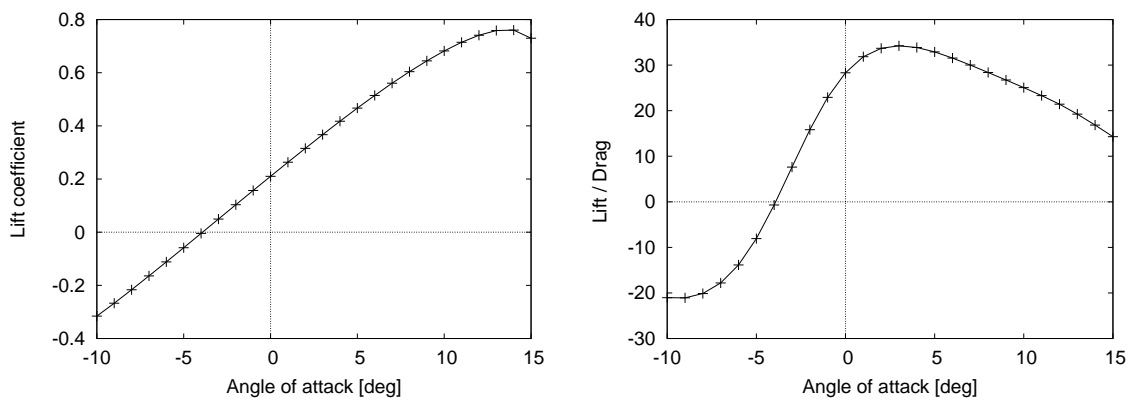


Figure 3.3: E-817 wing profile: Lift coefficient (left) and lift/drag ratio (right) in water, 5 knots

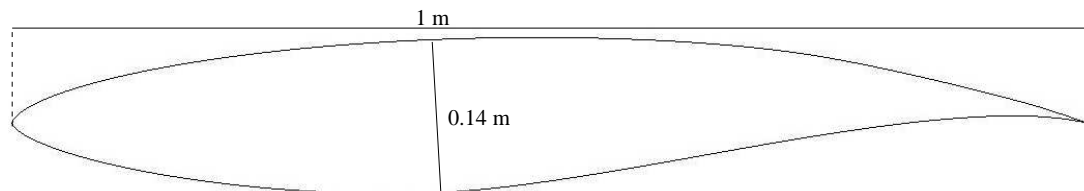


Figure 3.4: The SF-01 wing profile

### 3.2 The SF-01 wing profile

The SF-01 wing profile is shown in figure 3.4. This profile is designed at FFI and was introduced in [2].

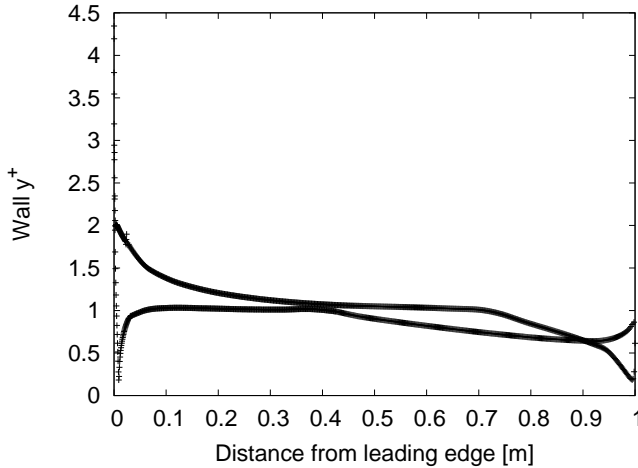


Figure 3.5: Calculated wall  $y^+$  for the SF-01 wing profile in water at  $5^\circ$  angle of attack

As in section 2.3, we check the grid quality in different ways. The calculated values of  $y^+$  at the first grid point from the wing at  $5^\circ$  angle of attack are shown in figure 3.5.

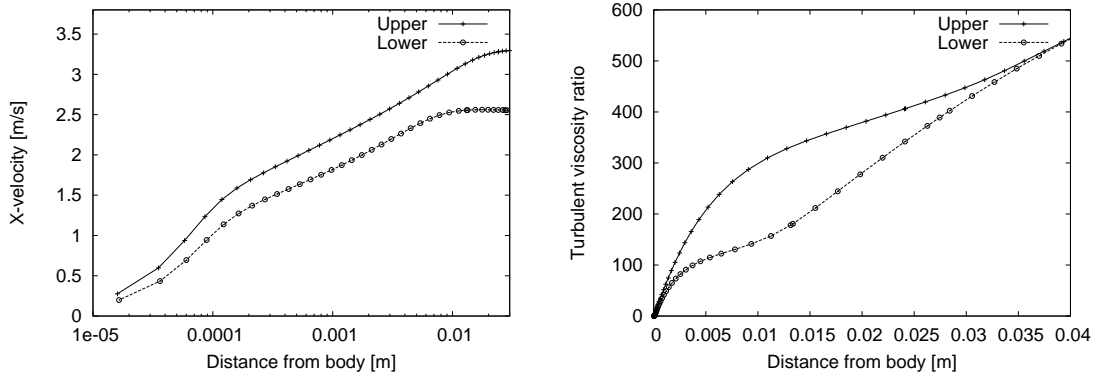


Figure 3.6: Horizontal velocity (left) and turbulent viscosity ratio (right) at  $x = 0.5$  for the SF-01 wing profile in water at  $5^\circ$  angle of attack

The horizontal velocity component and turbulent viscosity ratio along the line  $x = 0.5$  for the SF-01 wing profile at  $5^\circ$  angle of attack in water are shown in figure 3.6. These checks indicate that the grid is fine enough around the body.

Simulations are conducted for 5 knots speed in water ( $v_0 = 2.57$  m/s,  $Re = 2.56 \times 10^6$ , Mach  $1.7 \times 10^{-3}$ ,  $\rho_0 = 998.2$  kg/m<sup>3</sup>) with angle of attack varying from  $-10^\circ$  to  $15^\circ$ . Coefficients for moment, lift, drag, and lift/drag ratio are given in figures 3.7 and 3.8, and the results show the same trends as for the other two-dimensional profiles presented here.

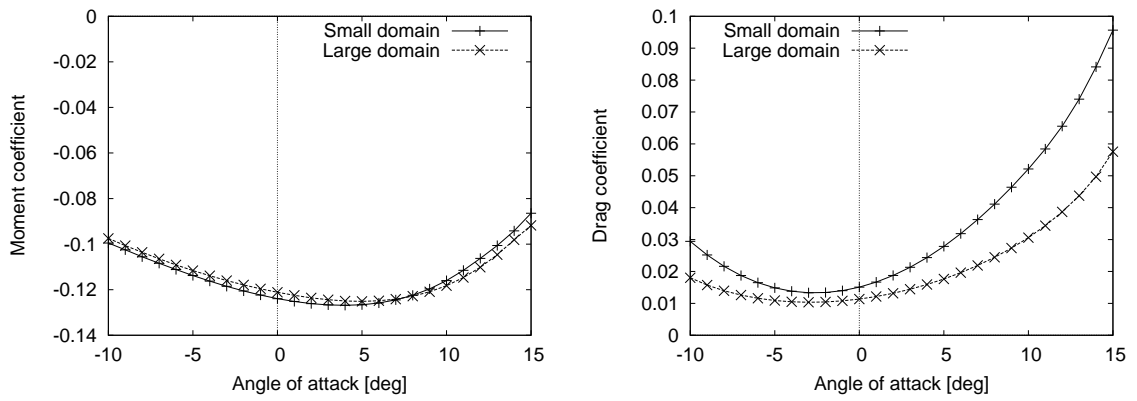


Figure 3.7: SF-01 wing profile: Moment (left) and drag (right) coefficients in water, 5 knots

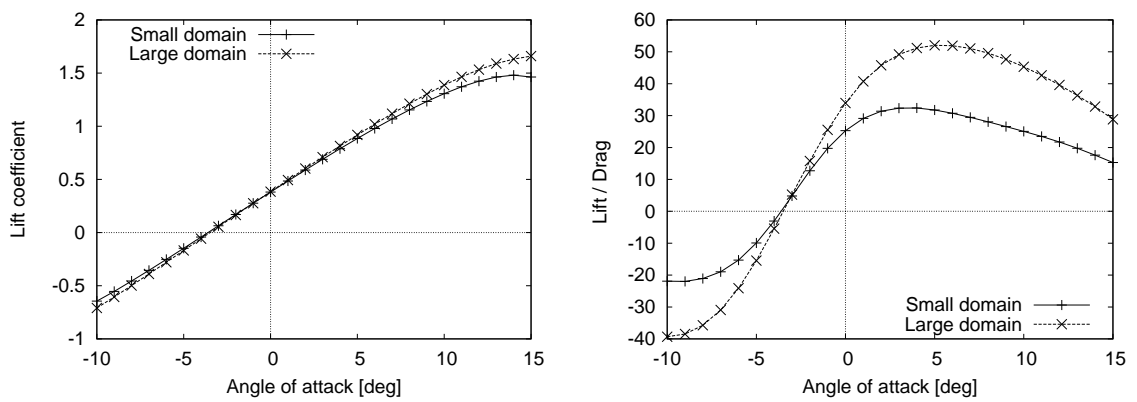


Figure 3.8: SF-01 wing profile: Lift coefficient (left) and lift/drag ratio (right) in water, 5 knots

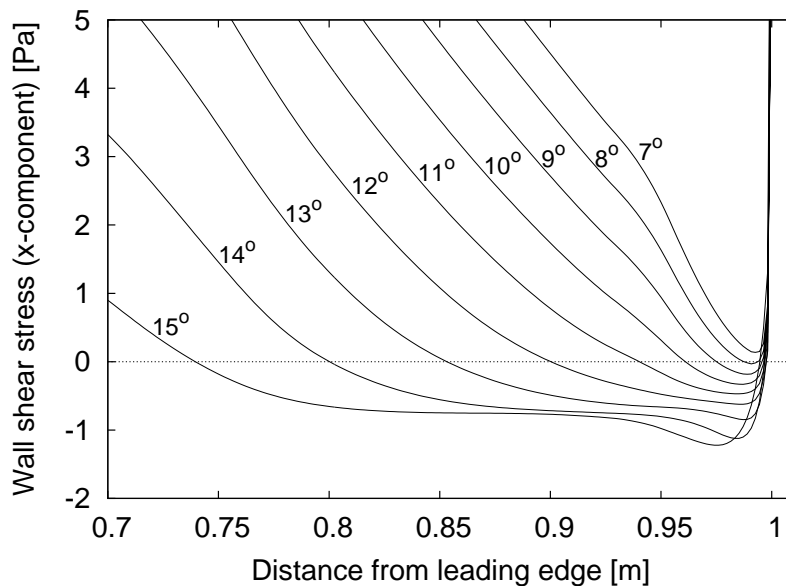
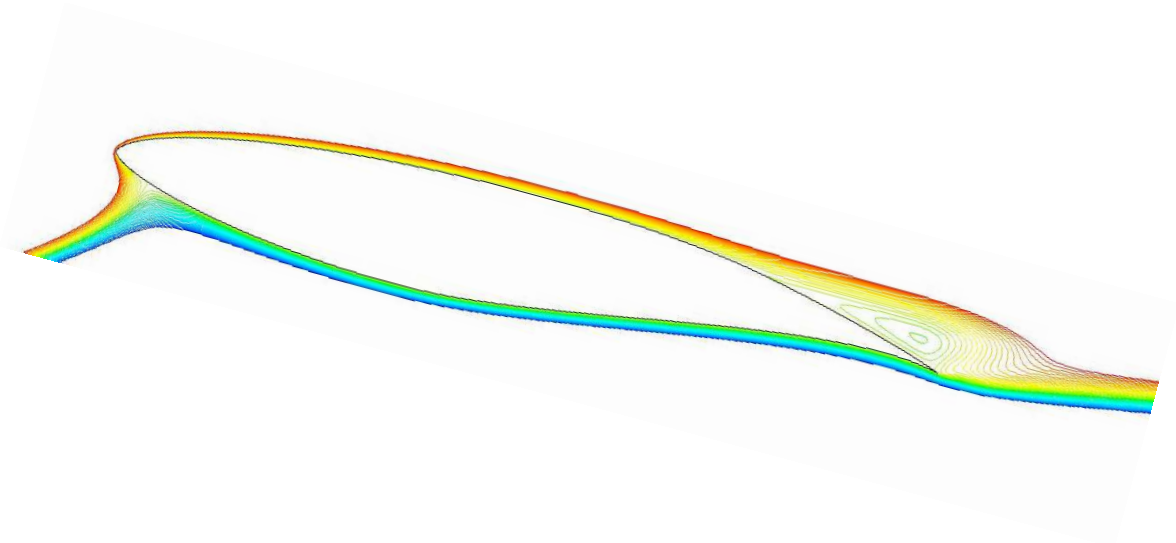


Figure 3.9: SF-01 wing profile: x-component of the wall shear stress along the suction side of the profile



*Figure 3.10: SF-01 wing profile: Separation at 15° angle of attack illustrated by the stream function. The contour lines of the stream function coincides with the streamlines*

Separation at the upper side of the profile occurs for angles of attack of 8° and larger. This is seen as negative  $x$ -component of the wall shear stress, shown in figure 3.9. A plot of the stream function, showing the separation, is given in figure 3.10.

## 4 Simulations of three-dimensional hydrofoils

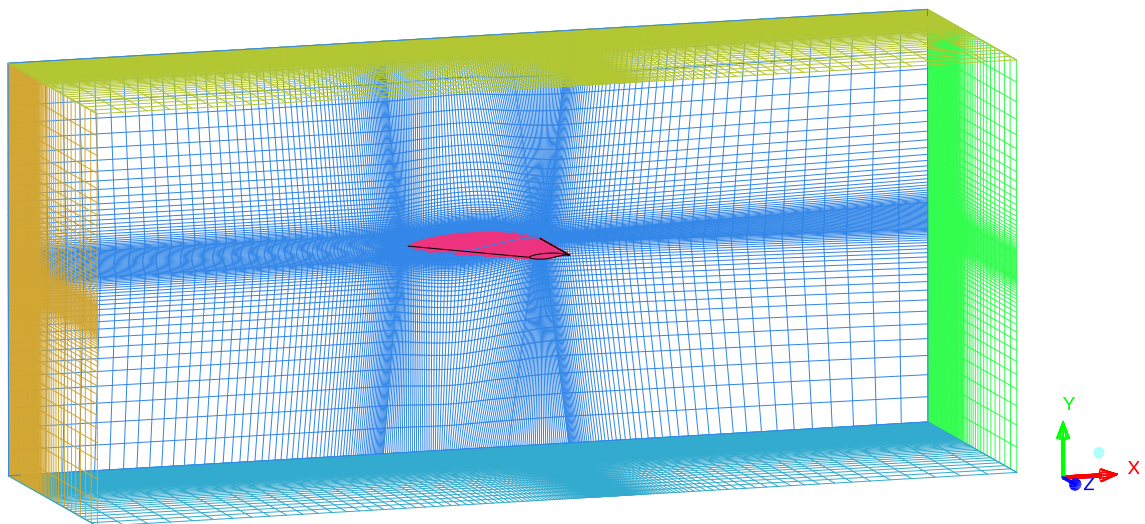


*Figure 4.1: Overview of the small computational domain and the grid structure in 3-d*

The three-dimensional simulations utilizes a symmetry plane in an  $xy$ -plane through the center of the wing (see figure 4.1). This choice is valid for steady computations without cross-flow, but makes

unsteady computations unphysical. As in two dimensions, two different domain sizes are used. The “small” domain is  $[-10,13] \times [-5,5] \times [0,7]$  m with 2.6 million hexahedral cells, while the “large” domain is  $[-20,50] \times [-20,20] \times [0,20]$  m with 14.1 million hexahedral cells. As in two dimensions, the grids for the small and large computational domains are identical in the region close to the wing. They are much coarser than the two-dimensional grid, as they have only 29 thousand and 102 thousand elements, respectively, in the symmetry plane, which corresponds to the two-dimensional computational domain. The thickness of the cells at the body surface in this case is 0.7–1 mm, i.e. 40–50 times larger than in the two-dimensional case.

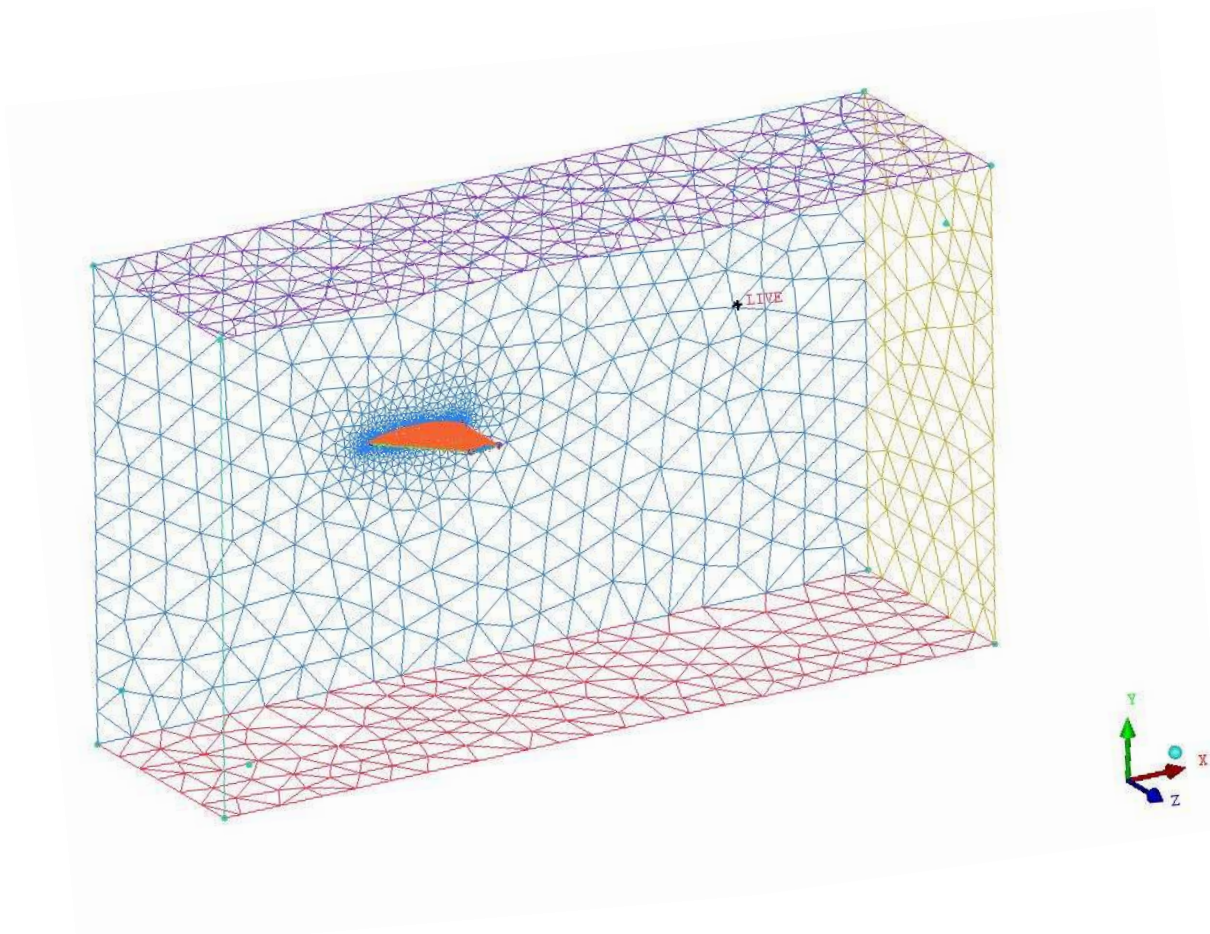


*Figure 4.2: Overview of the computational domain with the unstructured grid in 3-d*

Some results from simulations with an unstructured grid, taken from [2], are also included here. The domain for these simulations is  $[-9.8,17.9] \times [-7.9,7.9] \times [0,7.5]$  m with 632 thousand tetrahedral cells, i.e. closer to the small domain in size, and with far less grid cells. However, the thickness of the grid cells at the body surface is only  $20 \mu\text{m}$ . This domain with surface grids is shown in figure 4.2.

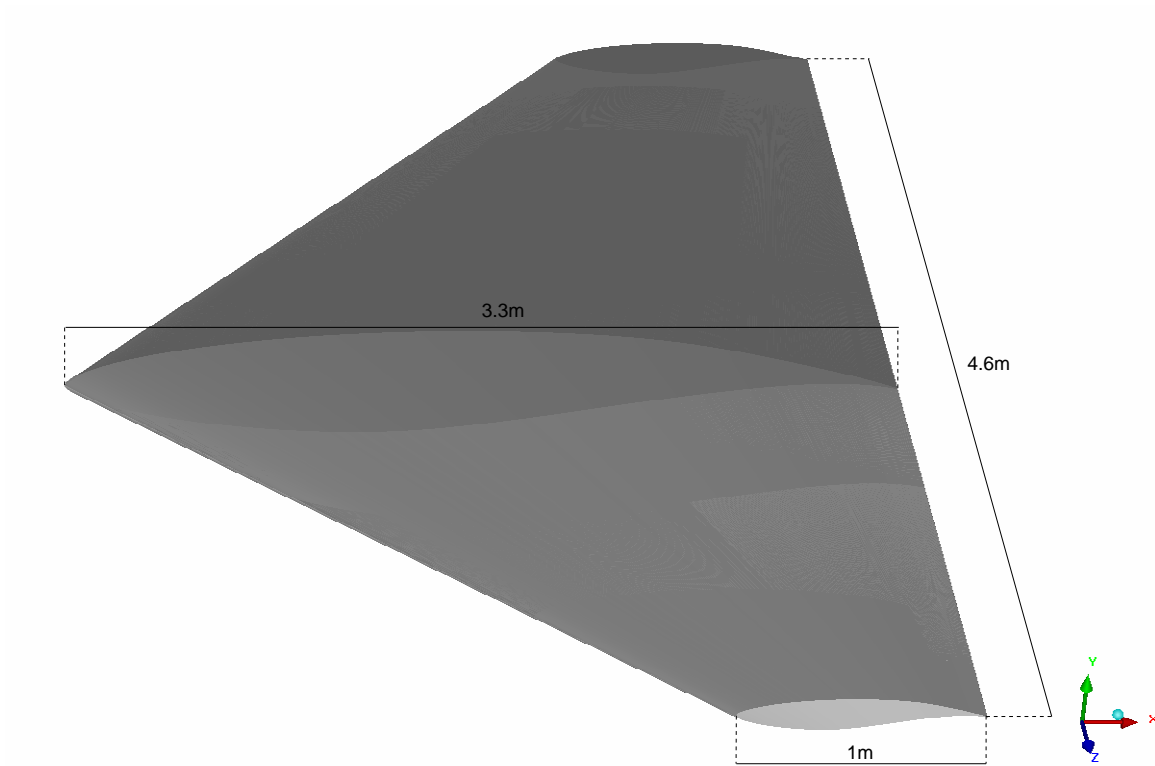


Figure 4.3: The SF-01-3D delta wing

#### 4.1 The SF-01-3D delta wing

The SF-01-3D delta wing is shown in figure 4.3. The wing uses the two-dimensional SF-01 profile, modified with a non-zero trailing edge thickness. The chord length is 3.3 m at the center and 1 m at the ends, and the span of the full wing is 4.6 m.

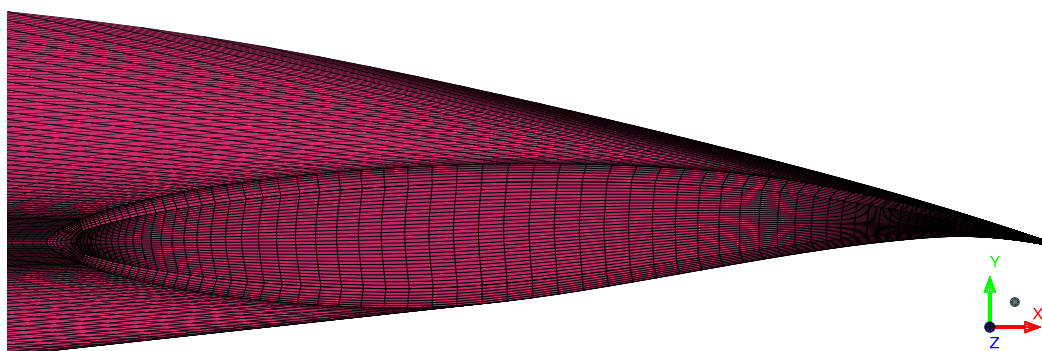


Figure 4.4: SF-01-3D wing, grid structure on wing tip profile

The new trailing edge changes the blocking strategy at the end of the profile. Sketches of the grid are shown in figures 4.4 (the wing tip) and 4.5 (the symmetry plane through the middle of the wing).



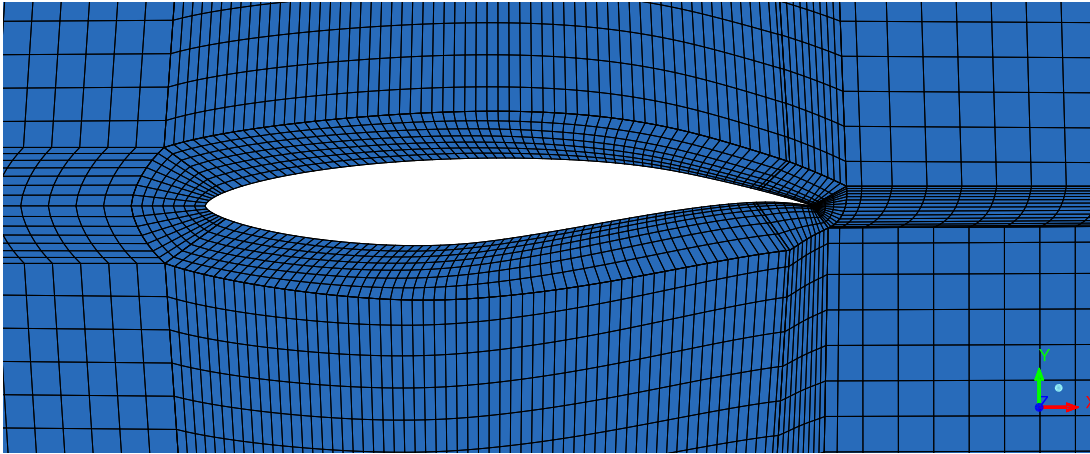


Figure 4.5: SF-01-3D wing, grid structure in the symmetry plane

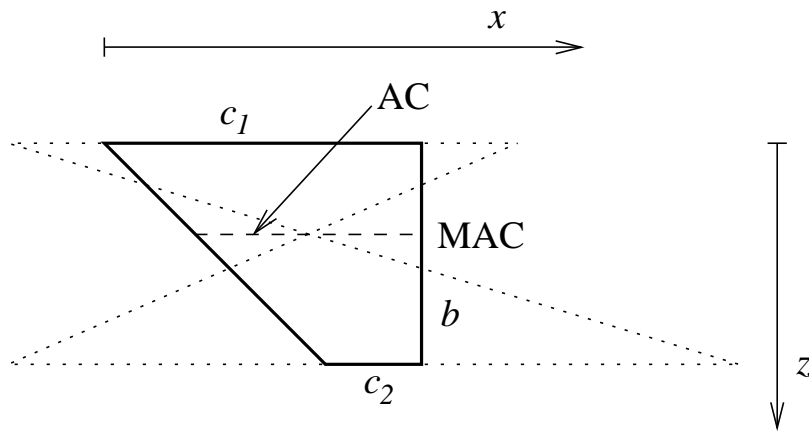


Figure 4.6: SF-01-3D wing: Mean aerodynamic chord line and centre

In two dimensions, the reference lengths and areas were the same for all the airfoils, and the moment centre was always taken to be at 25% of the chord length. For three-dimensional delta wings, the reference length is set to the centre chord length and the reference area to the projected area in the  $xz$ -plane (ref. figure 4.3).

The half-wing area is given by

$$A = \frac{(c_1 - c_2)b}{2} + c_2b,$$

which gives reference area  $A_0 = 2A = 9.89 \text{ m}^2$  for the SF-01-3D. The reference length is  $c_0 = c_1 = 3.3 \text{ m}$ .

To estimate the aerodynamic centre (AC), we consider half of the wing as shown in figure 4.6, and find the Mean Aerodynamic Chord (MAC) line. When the root chord length and tip chord length are denoted by  $c_1$  and  $c_2$ , respectively, and the wing span is  $b$ , the MAC line is placed at the crossing



of the lines

$$x = \frac{2c_1 + c_2}{b}z - c_2 \quad \text{and} \quad x = -\frac{c_1 + 2c_2}{b}z + c_1 + c_2,$$

which gives

$$z_{\text{MAC}} = \frac{b}{3} \frac{c_1 + 2c_2}{c_1 + c_2}.$$

The chord length is given by

$$c(z) = c_2 + \frac{c_1 - c_2}{b}(b - z),$$

so the MAC length is

$$c_{\text{MAC}} = c_2 + \frac{c_1 - c_2}{b}(b - z_{\text{MAC}}).$$

With  $c_1 = 3.3$  m,  $c_2 = 1$  m, and  $b = 2.3$  m, we obtain  $z_{\text{MAC}} = 0.9450$  m and  $c_{\text{MAC}} = 2.355$  m. Assuming that the aerodynamic centre (AC) is placed at 25% of the MAC length, we obtain  $x_{\text{AC}} = 1.534$  m.

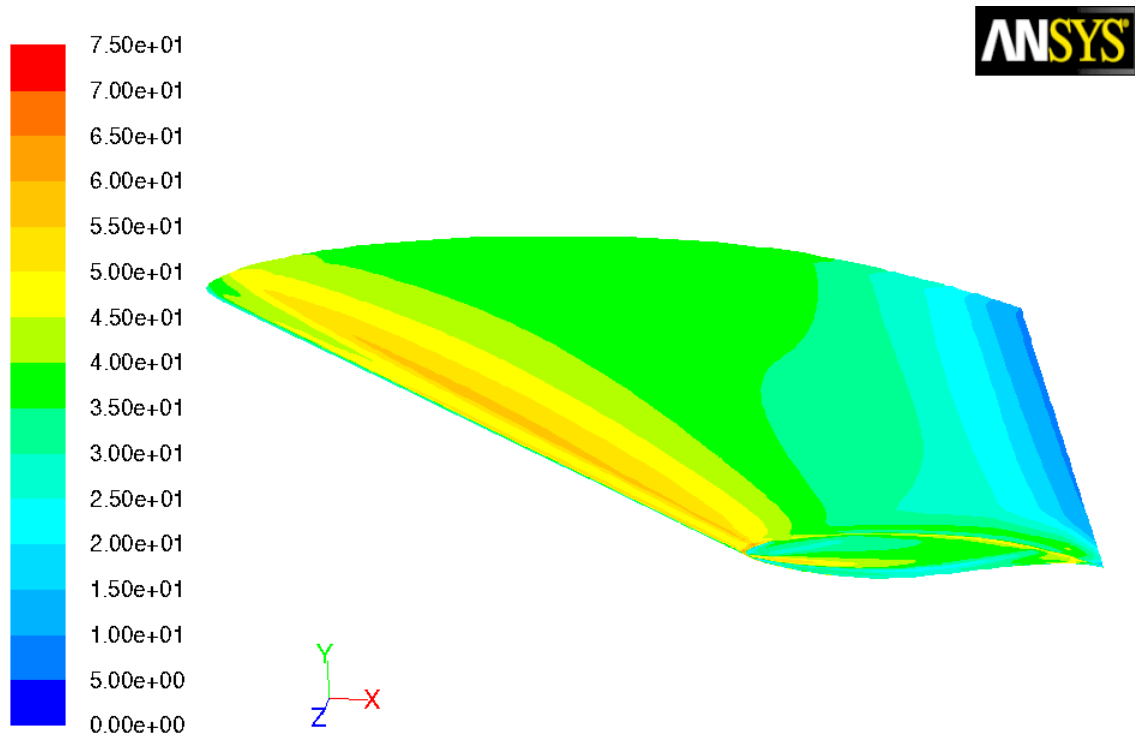


Figure 4.7: Calculated wall  $y^+$  for the SF-01-3D wing at  $5^\circ$  angle of attack in water, 5 knots, seen from above

To check the results, we first look at  $y^+$  at the first grid point away from the wing. This is shown in figures 4.7 and 4.8. We see that  $y^+$  is in the range 20–40 for the largest part of the wing surface. This is consistent with the two-dimensional results shown at the right side of figure 2.6, given the difference in the grid cell thickness at the body surface. This results in a different behaviour of the turbulence model, as the FLUENT implementation uses a log-law wall function when  $y^+ >$

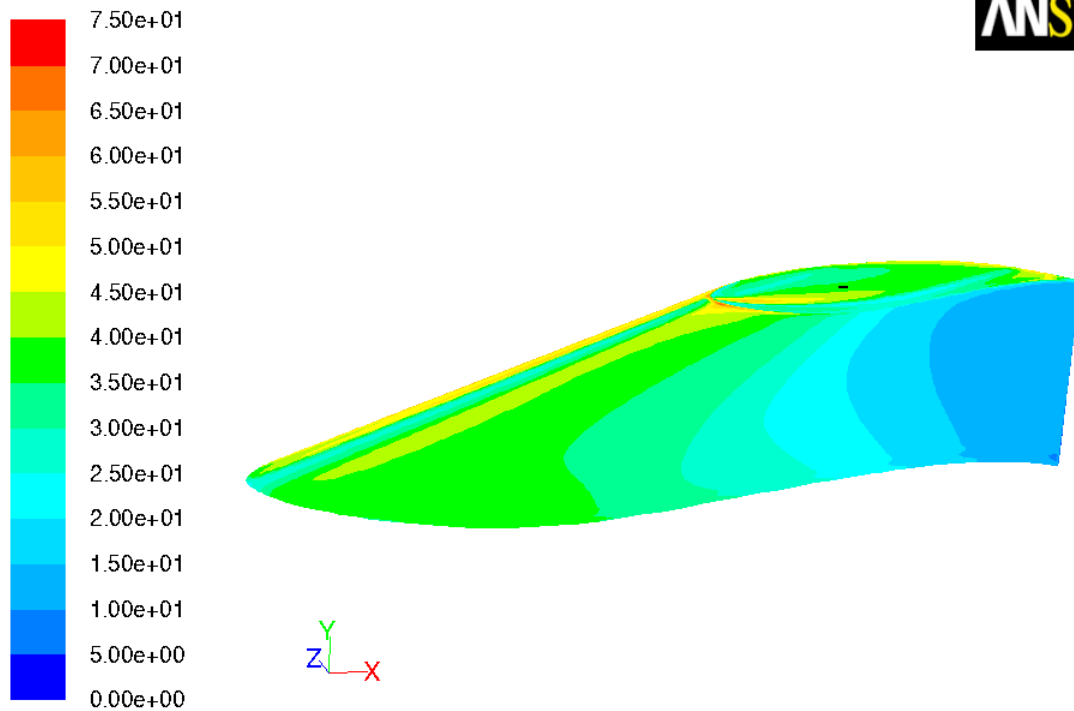


Figure 4.8: Calculated wall  $y^+$  for the SF-01-3D wing at  $5^\circ$  angle of attack in water, 5 knots, seen from below

11.225 [3]. According to [3], the log-law is valid for  $30 < y^+ < 300$ , so it is recommended that the first cell thickness corresponds to  $y^+ < 11$  or  $y^+ > 30$ . Note that a if the log-law is used, there may be problem when separation occurs. The calculated  $y^+$  at the first grid cell will decrease, which may cause the wall condition to switch from the log-law, and a stable solution may not be found if the condition keeps switching.

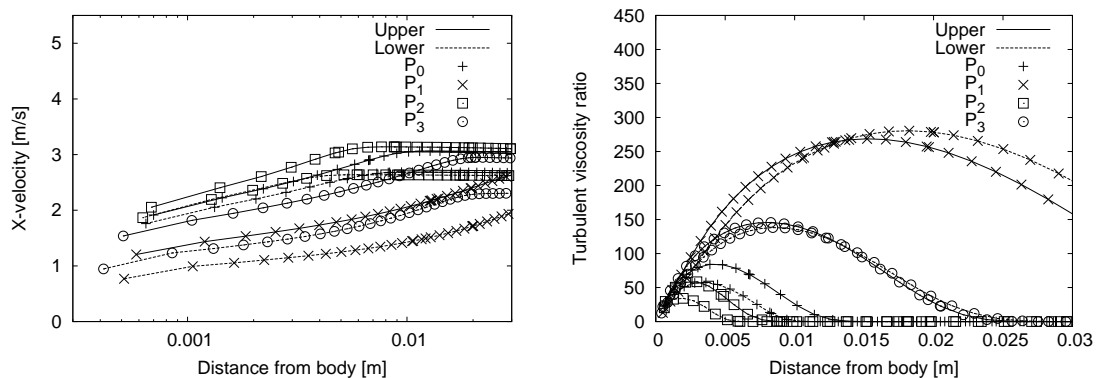


Figure 4.9: Horizontal velocity (left) and turbulent viscosity ratio (right) at  $x = 0.5$  for the SF-01-3D wing in water at  $5^\circ$  angle of attack, 5 knots

The horizontal velocity component and turbulent viscosity ratio at the  $(x, z)$ -values  $P_0 = (1.5, 1)$ ,  $P_1 = (3, 1)$ ,  $P_2 = (2.25, 2)$ , and  $P_3 = (3, 2)$  at  $5^\circ$  angle of attack in water are shown in figure 4.9. The smoothness of the curves indicate, as in two dimensions, that the grid resolution is sufficient around the body.

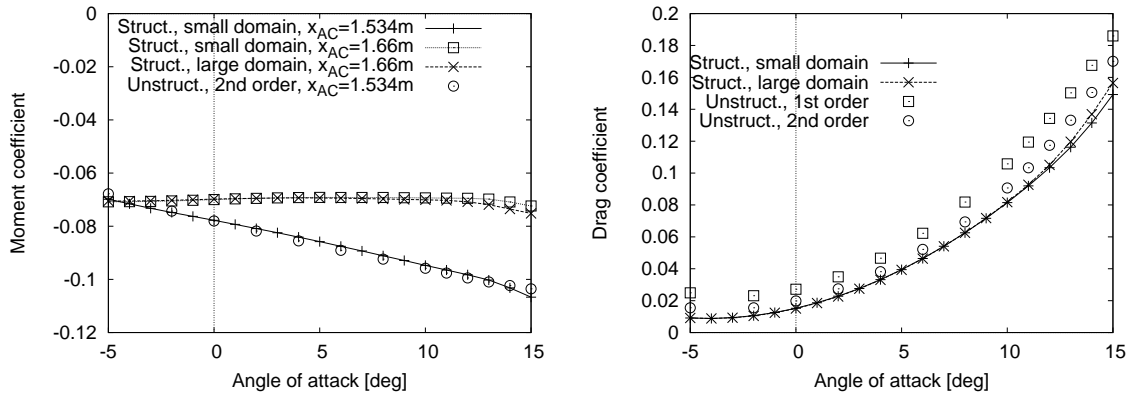


Figure 4.10: SF-01-3D wing: Moment (left) and drag (right) coefficients in water, 5 knots

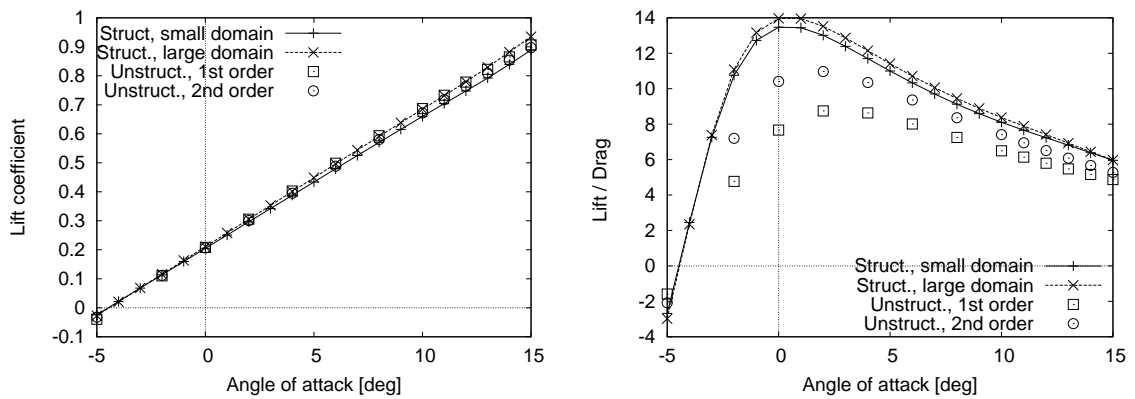


Figure 4.11: SF-01-3D wing: Lift coefficient (left) and lift/drag ratio (right) in water, 5 knots

Simulations are conducted for 5 knots speed in water ( $v_0 = 2.57$  m/s,  $Re = 2.56 \times 10^6$ , Mach  $1.7 \times 10^{-3}$ ,  $\rho_0 = 998.2$  kg/m<sup>3</sup>) with angle of attack varying from  $-5^\circ$  to  $15^\circ$ . Coefficients for moment, lift, drag, and lift/drag ratio are given in figures 4.10 and 4.11. The same simulations were also conducted for 3 knots speed on the small computational domain, and the coefficients are practically identical. As the coefficients are scaled by the reference velocity, this is expected within the same flow regime.

From figure 4.10 we notice that the estimate  $x_{AC} = 1.534$  m for the aerodynamic centre is erroneous. Numerical experiments show that  $x_{AC} = 1.66$  m gives a flatter moment curve for the SF01-3D wing, which suggests that this is a better choice. Another observation from these figures is that encouragingly good results are obtained on the unstructured grid. The unstructured grid is much more flexible than the structured grid, and is also easier to generate and gives faster calculations because of the coarser grid distribution away from the wing.

An important result from these simulations is that the influence of the domain size is small, even on the drag coefficients. This is a totally different behaviour from the two-dimensional case, as shown in section 2.3. Figure 4.10 also shows the importance of using second order spatial discretization, and not first order. The choice of discretization affects the drag coefficients more than the domain size in this case.

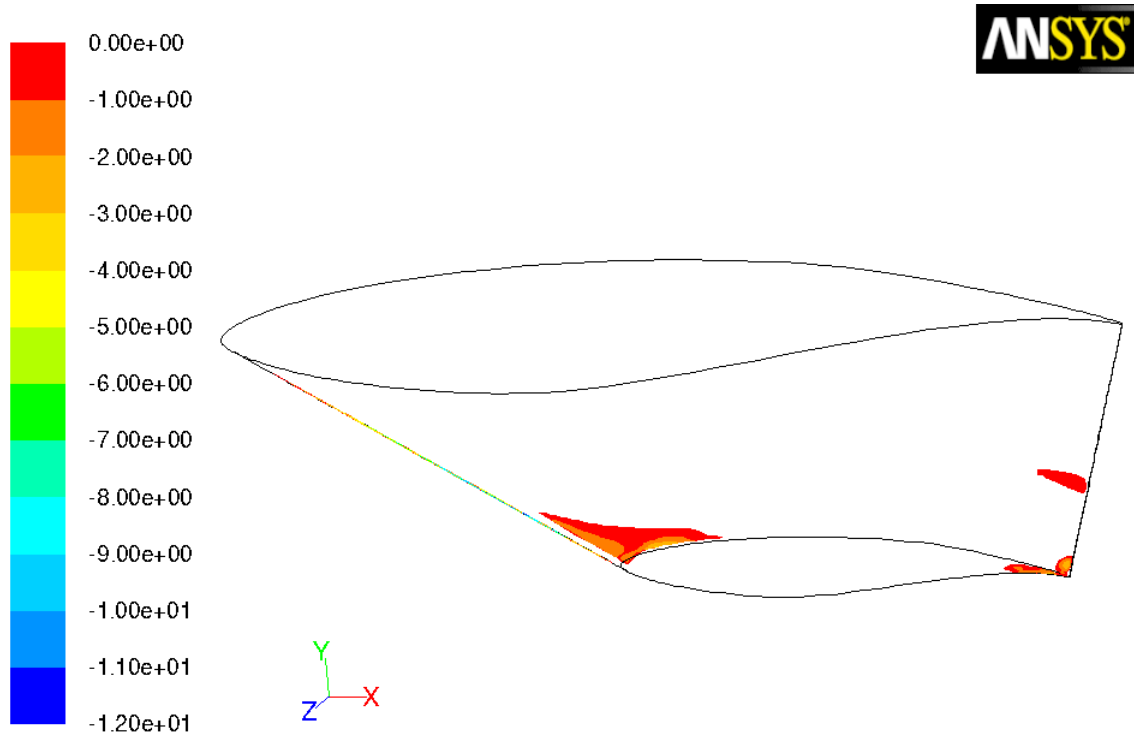


Figure 4.12: SF-01-3D wing: Negative values of the x-component of the wall shear stress at 15° angle of attack, 5 knots

In two dimensions, separation was observed for the SF-01 profile for angles of attack of 8° and larger. This is not seen in the present three-dimensional calculations. An illustration is given in figure 4.12, which only shows small areas of separation, mostly close to the wing tip, for an angle of attack of 15°. This may be attributed to the coarser grid close to the surfaces in the three-dimensional simulations.

## 4.2 The E-837-3D delta wing

The E-837-3D wing is shown in figure 4.13. This is a three-dimensional delta wing version of the two-dimensional Eppler profile E-837, again with the trailing edge of constant thickness 4 mm. The structured grid is constructed from the same blocking as for SF-01-3D, only changed to account for the increased dimensions of the wing. The computational domains are not changed.

By calculating the aerodynamic centre as described in section 4.1, we get  $x_{AC} = 1.9$  m, and the

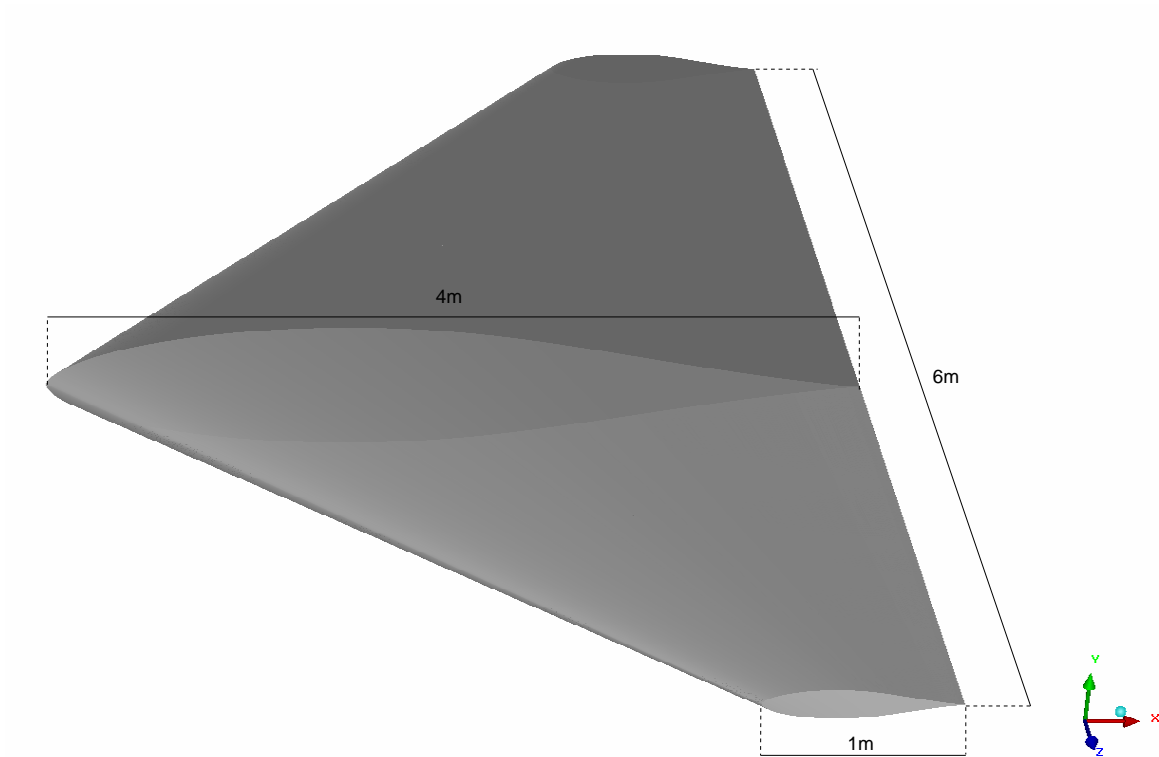


Figure 4.13: The E-837-3D wing

reference area for this wing is  $A_0 = 7.5 \text{ m}^2$ .

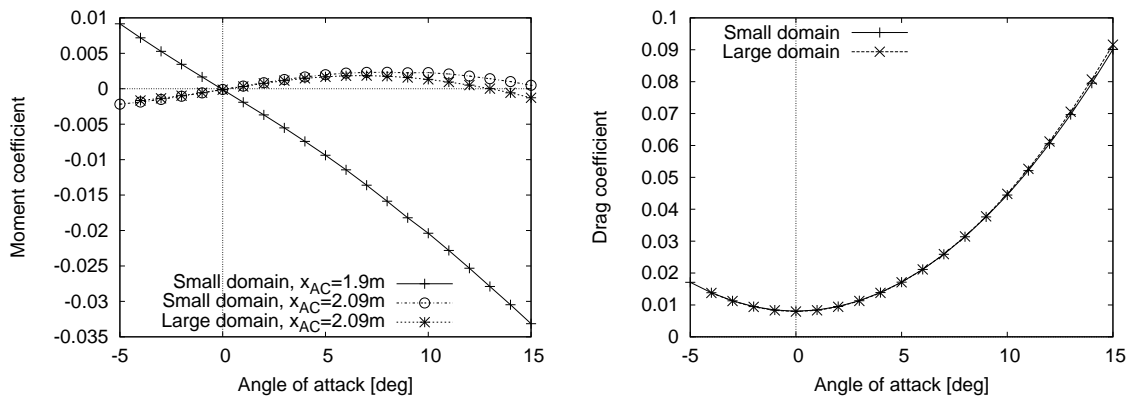


Figure 4.14: E-837-3D wing: Moment (left) and drag (right) coefficients in water, 5 knots

Simulations are conducted for 5 knots speed in water ( $v_0 = 2.57 \text{ m/s}$ ,  $Re = 2.56 \times 10^6$ , Mach  $1.7 \times 10^{-3}$ ,  $\rho_0 = 998.2 \text{ kg/m}^3$ ) with angle of attack varying from  $-5^\circ$  to  $15^\circ$ . Coefficients for moment, lift, drag, and lift/drag ratio are given in figures 4.14 and 4.15.

From figure 4.14 we notice that the estimate for the aerodynamic centre is not good enough. Numerical experiments show that  $x_{AC} = 2.09 \text{ m}$  gives a flatter moment curve for the E837-3D wing.

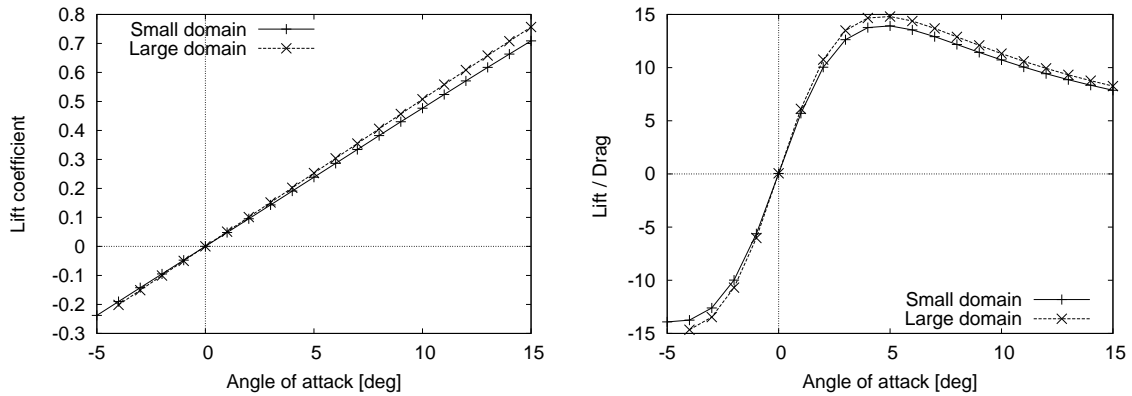


Figure 4.15: E-837-3D wing: Lift coefficient (left) and lift/drag ratio (right) in water, 5 knots

## 5 Conclusions and recommendations

A methodology for hydrodynamical simulations in FLUENT has been described, and applied to CFD analyses of two- and three-dimensional wings operating in air and water. The main output of the simulations are coefficients of lift, drag, and moment. Comparisons with reference data show good correspondence for lift and moment coefficients, whereas the drag coefficients depend on both the size of the computational domain and the turbulent flow conditions, as well as the discretization order.

The effect of the domain size has been investigated, and the obtained results are judged to be sufficiently accurate for the purposes of the underwater towing project. This effect has been found to be much smaller in three dimensions. Fully turbulent flow and flow with a laminar-turbulent transition have different friction drag properties, especially for small and moderate angles of attack, which makes direct comparisons with experimental data more difficult. However, the simulated drag coefficients are within the correct range, making the simulated results credible.

For large angles of attack, the flow is not necessarily steady, and the present steady-state simulations are not adequate. This means that stalling properties are not captured by these simulations and would require more elaborate simulations.

This report mainly describes simulations on structured hexahedral grids, but some comparisons are made with simulations on an unstructured grid with tetrahedral and prism cells. Encouragingly good results are obtained on the unstructured grid, which contains a factor 4 less cells than the structured grid for a comparable domain, and consequently yields much faster simulations.

Recommendations for hydrodynamical simulations:

- **Mathematical model:** The Navier-Stokes equations for viscous fluid flow give a good representation of the macroscopic flow. For hydrodynamical flow, an incompressible model is usually sufficient due to the high speed of sound and the low flow velocities. Without stratification, the fluid is defined as having constant density in FLUENT.

- The computational domain: The open boundaries, and particularly the outflow boundary must be placed sufficiently far away from the structures of interest. How far away that is depends on the simulation scenario and the accuracy requirements, but it is strongly recommended to test different domain sizes to be able to estimate the influence on the solution.
- The computational grid: The grid cells size at solid surfaces should be checked by calculating  $y^+$  at the surfaces from the simulation results. Check that the calculated  $y^+$  is consistent with the turbulence model, or that it is of order 1 for a direct numerical simulation (DNS), where no turbulence model is used. Be aware of special solution features, like separation, that can influence the calculation of  $y^+$ .
- Turbulence model: The Spalart-Allmaras RANS model is designed for external flows, but the wall-normal grid distribution close to solid surfaces should still be approximately of the same quality as for a DNS, i.e.  $y^+ \approx 1$  at the first grid point away from the wall.
- Boundary conditions: The type of boundary conditions must be consistent with the mathematical model and give a good representation of the physical situation.
- Convergence: Monitor forces, in addition to default convergence measures, during the simulation to judge whether the solution is numerically converged.
- Drag force calculations: As a general rule, the tendency is that both the use of low-order numerics and poor grid resolution near the walls will result in too large frictional forces, and consequently too high drag.
- Saved files: Save important files for all simulations, so the simulation can be recreated or re-examined. A minimum is a FLUENT case file (containing the grid and all settings), a data file with the solution at the end of the simulation, and a data file with the initial condition, if this is non-trivial and not computed from the boundary conditions. FLUENT input report files, as included in the Appendix, are generated from the case file.

## References

- [1] Ira H. Abbott and Albert E. Von Doenhoff. *Theory of wing sections*. Dover Publications Inc., New York, 1959.
- [2] Øyvind Andreassen, Øyvind Grandum, Jan Charles Kielland, Kjetill Løvbrøtte, Bjørn Anders Pettersson Reif, and Carl Erik Wasberg. Hydrodynamic design and analysis of tail fish. Technical Report 2010/00136, FFI, 2010. UNNTATT OFFENTLIGHET.
- [3] ANSYS Inc. *ANSYS FLUENT 12.0 Theory Guide*, 2009.
- [4] NASA Langley Research Center. Turbulence modeling resource. Web page. <http://turbmodels.larc.nasa.gov/>.

- [5] P. Spalart and S. Allmaras. A one-equation turbulence model for aerodynamic flows. *AIAA Paper*, pages 92–0439, 1992.



## Appendix A FLUENT reports

All input settings for a FLUENT simulation can be reported to a summary-file (.sum). It is highly recommended to save a summary file for each simulation. This appendix contains the input reports for the simulation of NACA-0009 in air, SF-01 in water, and SF-01-3D in water, all taken at 5° angle of attack.

### A.1 FLUENT input report for NACA-0009 in air

FLUENT  
Version: 2d, dp, pbns, S-A (2d, double precision, pressure-based,  
Spalart-Allmaras)  
Release: 12.0.16  
Title:

#### Models

Model	Settings
Space	2D
Time	Steady
Viscous	Spalart-Allmaras turbulence model
Production Option	Vorticity
Heat Transfer	Disabled
Solidification and Melting	Disabled
Species Transport	Disabled
Coupled Dispersed Phase	Disabled
Pollutants	Disabled
Pollutants	Disabled
Soot	Disabled

#### Material Properties

Material: air (fluid)

Property	Units	Method	Value(s)
Density	kg/m3	constant	1.225
Cp (Specific Heat)	j/kg-k	constant	1006.43
Thermal Conductivity	w/m-k	constant	0.0242
Viscosity	kg/m-s	constant	1.7894e-05
Molecular Weight	kg/kgmol	constant	28.966
Thermal Expansion Coefficient	1/k	constant	0
Speed of Sound	m/s	none	#f

Material: aluminum (solid)

Property	Units	Method	Value(s)
Density	kg/m3	constant	2719
Cp (Specific Heat)	j/kg-k	constant	871
Thermal Conductivity	w/m-k	constant	202.4

#### Cell Zone Conditions

##### Zones

name	id	type
solid	16	fluid

##### Setup Conditions

solid

Condition	Value
Material Name	air
Specify source terms?	no
Source Terms	((mass) (x-momentum) (y-momentum) (nut))
Specify fixed values?	no
Fixed Values	((x-velocity (inactive . #f) (constant . 0) (profile )) (y-velocity (inactive . #f) (constant . 0) (profile )) (nut (inactive . #f) (constant . 0) (profile )))
Motion Type	0
X-Velocity Of Zone (m/s)	0
Y-Velocity Of Zone (m/s)	0
Rotation speed (rad/s)	0
X-Origin of Rotation-Axis (m)	0
Y-Origin of Rotation-Axis (m)	0
Deactivated Thread	no
Laminar zone?	no
Set Turbulent Viscosity to zero within laminar zone?	yes
Porous zone?	no
X-Component of Direction-1 Vector	1
Y-Component of Direction-1 Vector	0
Relative Velocity Resistance Formulation?	yes
Direction-1 Viscous Resistance (1/m <sup>2</sup> )	0
Direction-2 Viscous Resistance (1/m <sup>2</sup> )	0
Choose alternative formulation for inertial resistance?	no
Direction-1 Inertial Resistance (1/m)	0
Direction-2 Inertial Resistance (1/m)	0
C0 Coefficient for Power-Law	0
C1 Coefficient for Power-Law	0
Porosity	1

#### Boundary Conditions

##### Zones

name	id	type
inlet	18	velocity-inlet
outlet	19	outflow
body	24	wall
top	20	periodic
bottom	22	periodic

##### Setup Conditions

###### inlet

Condition	Value
Velocity Specification Method	0
Reference Frame	0
Velocity Magnitude (m/s)	102.9
X-Velocity (m/s)	0
Y-Velocity (m/s)	0
X-Component of Flow Direction	0.9961947
Y-Component of Flow Direction	0.0871557
X-Component of Axis Direction	0
Y-Component of Axis Direction	0
Z-Component of Axis Direction	1
X-Coordinate of Axis Origin (m)	0
Y-Coordinate of Axis Origin (m)	0
Z-Coordinate of Axis Origin (m)	0
Angular velocity (rad/s)	0
Turbulent Specification Method	2
Modified Turbulent Viscosity (m <sup>2</sup> /s)	0.001
Turbulent Intensity (%)	10
Turbulent Length Scale (m)	1
Hydraulic Diameter (m)	1

Turbulent Viscosity Ratio 1  
 is zone used in mixing-plane model? no

outlet

Condition	Value
Flow rate weighting	1

body

Condition	Value
Wall Motion	0
Shear Boundary Condition	0
Define wall motion relative to adjacent cell zone?	yes
Apply a rotational velocity to this wall?	no
Velocity Magnitude (m/s)	0
X-Component of Wall Translation	1
Y-Component of Wall Translation	0
Define wall velocity components?	no
X-Component of Wall Translation (m/s)	0
Y-Component of Wall Translation (m/s)	0
Wall Roughness Height (m)	0
Wall Roughness Constant	0.5
Rotation Speed (rad/s)	0
X-Position of Rotation-Axis Origin (m)	0
Y-Position of Rotation-Axis Origin (m)	0
X-component of shear stress (pascal)	0
Y-component of shear stress (pascal)	0
Specularity Coefficient	0

top

Condition	Value
Rotationally Periodic?	no

bottom

Condition	Value
Rotationally Periodic?	no

#### Solver Settings

##### Equations

Equation	Solved
Flow	yes
Modified Turbulent Viscosity	yes

##### Numerics

Numeric	Enabled
Absolute Velocity Formulation	yes

##### Relaxation

Variable	Relaxation Factor
Pressure	0.3
Density	1
Body Forces	1
Momentum	0.7
Modified Turbulent Viscosity	0.8
Turbulent Viscosity	1

##### Linear Solver

Variable	Solver Type	Termination Criterion	Residual Reduction Tolerance
----------	-------------	-----------------------	------------------------------

```

-----
Pressure           V-Cycle    0.1
X-Momentum        Flexible   0.1          0.7
Y-Momentum        Flexible   0.1          0.7
Modified Turbulent Viscosity Flexible   0.1          0.7

Pressure-Velocity Coupling

Parameter  Value
-----
Type      SIMPLE

Discretization Scheme

Variable           Scheme
-----
Pressure          Standard
Momentum          Second Order Upwind
Modified Turbulent Viscosity Second Order Upwind

Solution Limits

Quantity           Limit
-----
Minimum Absolute Pressure  1
Maximum Absolute Pressure  5e+10
Minimum Temperature        1
Maximum Temperature        5000
Maximum Turb. Viscosity Ratio 100000

```

## A.2 FLUENT input report for SF-01 in water

```

FLUENT
Version: 2d, dp, pbns, S-A (2d, double precision, pressure-based,
Spalart-Allmaras)
Release: 12.0.16
Title:

```

### Models

```

-----
Model           Settings
-----
Space          2D
Time           Steady
Viscous        Spalart-Allmaras turbulence model
Production Option Vorticity
Heat Transfer  Disabled
Solidification and Melting Disabled
Species Transport Disabled
Coupled Dispersed Phase Disabled
Pollutants     Disabled
Pollutants     Disabled
Soot           Disabled

```

### Material Properties

```

Material: water-liquid (fluid)

```

Property	Units	Method	Value(s)
Density	kg/m3	constant	998.20001
Cp (Specific Heat)	j/kg-k	constant	4182
Thermal Conductivity	w/m-k	constant	0.6
Viscosity	kg/m-s	constant	0.001003
Molecular Weight	kg/kgmol	constant	18.0152
Thermal Expansion Coefficient	1/k	constant	0
Speed of Sound	m/s	none	#f

```

Material: air (fluid)

```

Property	Units	Method	Value(s)
----------	-------	--------	----------

```

-----
Density                kg/m3      constant  1.225
Cp (Specific Heat)    j/kg-k    constant  1006.43
Thermal Conductivity  w/m-k     constant  0.0242
Viscosity              kg/m-s    constant  1.7894e-05
Molecular Weight      kg/kgmol  constant  28.966
Thermal Expansion Coefficient  1/k      constant  0
Speed of Sound        m/s       none     #f

```

Material: aluminum (solid)

```

Property              Units      Method    Value(s)
-----
Density                kg/m3     constant  2719
Cp (Specific Heat)    j/kg-k    constant  871
Thermal Conductivity  w/m-k     constant  202.4

```

Cell Zone Conditions

Zones

```

name    id    type
-----
solid   21    fluid

```

Setup Conditions

solid

```

Condition              Value
-----
Material Name          water-liquid
Specify source terms? no
Source Terms           ((mass) (x-momentum)
                       (y-momentum) (nut))
Specify fixed values? no
Fixed Values           ((x-velocity (inactive . #f)
                       (constant . 0) (profile ))
                       (y-velocity (inactive . #f)
                       (constant . 0) (profile ))
                       (nut (inactive . #f)
                       (constant . 0) (profile )))
Motion Type            0
X-Velocity Of Zone (m/s) 0
Y-Velocity Of Zone (m/s) 0
Rotation speed (rad/s)  0
X-Origin of Rotation-Axis (m) 0
Y-Origin of Rotation-Axis (m) 0
Deactivated Thread     no
Laminar zone?         no
Set Turbulent Viscosity to zero within
laminar zone?         yes
Porous zone?          no
X-Component of Direction-1 Vector 1
Y-Component of Direction-1 Vector 0
Relative Velocity Resistance Formulation? yes
Direction-1 Viscous Resistance (1/m2) 0
Direction-2 Viscous Resistance (1/m2) 0
Choose alternative formulation for
inertial resistance?  no
Direction-1 Inertial Resistance (1/m) 0
Direction-2 Inertial Resistance (1/m) 0
C0 Coefficient for Power-Law 0
C1 Coefficient for Power-Law 0
Porosity               1

```

Boundary Conditions

Zones

```

name    id    type
-----
outlet  24    outflow
inlet   23    velocity-inlet

```

```

body      29    wall
top       25    periodic
bottom    27    periodic

```

Setup Conditions

outlet

```

Condition          Value
-----
Flow rate weighting  1

```

inlet

```

Condition          Value
-----
Velocity Specification Method  0
Reference Frame          0
Velocity Magnitude (m/s)     2.57
X-Velocity (m/s)          0
Y-Velocity (m/s)          0
X-Component of Flow Direction  0.9961947
Y-Component of Flow Direction  0.087155742
X-Component of Axis Direction  0
Y-Component of Axis Direction  0
Z-Component of Axis Direction  1
X-Coordinate of Axis Origin (m)  0
Y-Coordinate of Axis Origin (m)  0
Z-Coordinate of Axis Origin (m)  0
Angular velocity (rad/s)      0
Turbulent Specification Method  0
Modified Turbulent Viscosity (m2/s)  0.001
Turbulent Intensity (%)      10
Turbulent Length Scale (m)    1
Hydraulic Diameter (m)        1
Turbulent Viscosity Ratio     10
is zone used in mixing-plane model?  no

```

body

```

Condition          Value
-----
Wall Motion          0
Shear Boundary Condition  0
Define wall motion relative to adjacent cell zone?  yes
Apply a rotational velocity to this wall?  no
Velocity Magnitude (m/s)    0
X-Component of Wall Translation  1
Y-Component of Wall Translation  0
Define wall velocity components?  no
X-Component of Wall Translation (m/s)  0
Y-Component of Wall Translation (m/s)  0
Wall Roughness Height (m)    0
Wall Roughness Constant     0.5
Rotation Speed (rad/s)      0
X-Position of Rotation-Axis Origin (m)  0
Y-Position of Rotation-Axis Origin (m)  0
X-component of shear stress (pascal)  0
Y-component of shear stress (pascal)  0
Specularity Coefficient     0

```

top

```

Condition          Value
-----
Rotationally Periodic?  no

```

bottom

```

Condition          Value
-----
Rotationally Periodic?  no

```

Solver Settings

-----

Equations

Equation	Solved
Flow	yes
Modified Turbulent Viscosity	yes

Numerics

Numeric	Enabled
Absolute Velocity Formulation	yes

Relaxation

Variable	Relaxation Factor
Pressure	0.3
Density	1
Body Forces	1
Momentum	0.7
Modified Turbulent Viscosity	0.8
Turbulent Viscosity	1

Linear Solver

Variable	Solver Type	Termination Criterion	Residual Reduction Tolerance
Pressure	V-Cycle	0.1	
X-Momentum	Flexible	0.1	0.7
Y-Momentum	Flexible	0.1	0.7
Modified Turbulent Viscosity	Flexible	0.1	0.7

Pressure-Velocity Coupling

Parameter	Value
Type	SIMPLE

Discretization Scheme

Variable	Scheme
Pressure	Standard
Momentum	Second Order Upwind
Modified Turbulent Viscosity	Second Order Upwind

Solution Limits

Quantity	Limit
Minimum Absolute Pressure	1
Maximum Absolute Pressure	5e+10
Minimum Temperature	1
Maximum Temperature	5000
Maximum Turb. Viscosity Ratio	100000

### A.3 FLUENT input report for SF-01-3D in water

FLUENT  
Version: 3d, dp, pbns, S-A (3d, double precision, pressure-based, Spalart-Allmaras)  
Release: 12.0.16  
Title:

Models

Model	Settings
Space	3D
Time	Steady

```

Viscous                               Spalart-Allmaras turbulence model
Production Option                      Vorticity
Heat Transfer                          Disabled
Solidification and Melting             Disabled
Species Transport                      Disabled
Coupled Dispersed Phase               Disabled
Pollutants                            Disabled
Pollutants                            Disabled
Soot                                   Disabled

```

Material Properties

Material: water-liquid (fluid)

Property	Units	Method	Value(s)
Density	kg/m3	constant	998.2
Cp (Specific Heat)	j/kg-k	constant	4182
Thermal Conductivity	w/m-k	constant	0.6
Viscosity	kg/m-s	constant	0.001003
Molecular Weight	kg/kgmol	constant	18.0152
Thermal Expansion Coefficient	1/k	constant	0
Speed of Sound	m/s	none	#f

Material: air (fluid)

Property	Units	Method	Value(s)
Density	kg/m3	constant	1.225
Cp (Specific Heat)	j/kg-k	constant	1006.43
Thermal Conductivity	w/m-k	constant	0.0242
Viscosity	kg/m-s	constant	1.7894e-05
Molecular Weight	kg/kgmol	constant	28.966
Thermal Expansion Coefficient	1/k	constant	0
Speed of Sound	m/s	none	#f

Material: aluminum (solid)

Property	Units	Method	Value(s)
Density	kg/m3	constant	2719
Cp (Specific Heat)	j/kg-k	constant	871
Thermal Conductivity	w/m-k	constant	202.4

Cell Zone Conditions

Zones

name	id	type
solid	10057	fluid

Setup Conditions

solid

Condition	Value
Material Name	water-liquid
Specify source terms?	no
Source Terms	((mass) (x-momentum) (y-momentum) (z-momentum) (nut))
Specify fixed values?	no
Local Coordinate System for Fixed Velocities	no
Fixed Values	((x-velocity (inactive . #f) (constant . 0) (profile )) (y-velocity (inactive . #f) (constant . 0) (profile )) (z-velocity (inactive . #f) (constant . 0) (profile )) (nut (inactive . #f))



```

                                                                    (constant . 0) (profile )))
Motion Type                                                            0
X-Velocity Of Zone (m/s)                                             0
Y-Velocity Of Zone (m/s)                                             0
Z-Velocity Of Zone (m/s)                                             0
Rotation speed (rad/s)                                               0
X-Origin of Rotation-Axis (m)                                        0
Y-Origin of Rotation-Axis (m)                                        0
Z-Origin of Rotation-Axis (m)                                        0
X-Component of Rotation-Axis                                         0
Y-Component of Rotation-Axis                                         0
Z-Component of Rotation-Axis                                         1
Deactivated Thread                                                  no
Laminar zone?                                                        no
Set Turbulent Viscosity to zero within
laminar zone?                                                        yes
Porous zone?                                                         no
Conical porous zone?                                                no
X-Component of Direction-1 Vector                                    1
Y-Component of Direction-1 Vector                                    0
Z-Component of Direction-1 Vector                                    0
X-Component of Direction-2 Vector                                    0
Y-Component of Direction-2 Vector                                    1
Z-Component of Direction-2 Vector                                    0
X-Component of Cone Axis Vector                                      1
Y-Component of Cone Axis Vector                                      0
Z-Component of Cone Axis Vector                                      0
X-Coordinate of Point on Cone Axis (m)                              1
Y-Coordinate of Point on Cone Axis (m)                              0
Z-Coordinate of Point on Cone Axis (m)                              0
Half Angle of Cone Relative to its
Axis (deg)                                                            0
Relative Velocity Resistance Formulation?                            yes
Direction-1 Viscous Resistance (1/m2)                               0
Direction-2 Viscous Resistance (1/m2)                               0
Direction-3 Viscous Resistance (1/m2)                               0
Choose alternative formulation for
inertial resistance?                                                no
Direction-1 Inertial Resistance (1/m)                               0
Direction-2 Inertial Resistance (1/m)                               0
Direction-3 Inertial Resistance (1/m)                               0
C0 Coefficient for Power-Law                                         0
C1 Coefficient for Power-Law                                         0
Porosity                                                              1

```

#### Boundary Conditions

-----

#### Zones

name	id	type
symmetry	10064	symmetry
outlet	52	outflow
outer	10063	velocity-inlet
inlet	53	velocity-inlet
body	10059	wall
top	54	periodic

#### Setup Conditions

##### symmetry

Condition	Value
-----	

##### outlet

Condition	Value
-----	
Flow rate weighting	1

##### outer

Condition	Value

```

-----
Velocity Specification Method      0
Reference Frame                    0
Velocity Magnitude (m/s)         2.5722
Coordinate System                  0
X-Velocity (m/s)                  0
Y-Velocity (m/s)                  0
Z-Velocity (m/s)                  0
X-Component of Flow Direction     0.9961947
Y-Component of Flow Direction     0.0871557
Z-Component of Flow Direction     0
X-Component of Axis Direction     0
Y-Component of Axis Direction     0
Z-Component of Axis Direction     1
X-Coordinate of Axis Origin (m)   0
Y-Coordinate of Axis Origin (m)   0
Z-Coordinate of Axis Origin (m)   0
Angular velocity (rad/s)          0
Turbulent Specification Method    0
Modified Turbulent Viscosity (m2/s) 0.001
Turbulent Intensity (%)           10
Turbulent Length Scale (m)        1
Hydraulic Diameter (m)            1
Turbulent Viscosity Ratio         1
is zone used in mixing-plane model? no

```

inlet

```

Condition                          Value
-----
Velocity Specification Method      0
Reference Frame                    0
Velocity Magnitude (m/s)         2.5722
Coordinate System                  0
X-Velocity (m/s)                  0
Y-Velocity (m/s)                  0
Z-Velocity (m/s)                  0
X-Component of Flow Direction     0.9961947
Y-Component of Flow Direction     0.0871557
Z-Component of Flow Direction     0
X-Component of Axis Direction     1
Y-Component of Axis Direction     0
Z-Component of Axis Direction     0
X-Coordinate of Axis Origin (m)   0
Y-Coordinate of Axis Origin (m)   0
Z-Coordinate of Axis Origin (m)   0
Angular velocity (rad/s)          0
Turbulent Specification Method    0
Modified Turbulent Viscosity (m2/s) 0.001
Turbulent Intensity (%)           10
Turbulent Length Scale (m)        1
Hydraulic Diameter (m)            1
Turbulent Viscosity Ratio         1
is zone used in mixing-plane model? no

```

body

```

Condition                          Value
-----
Enable shell conduction?          no
Wall Motion                        0
Shear Boundary Condition           0
Define wall motion relative to adjacent cell zone? yes
Apply a rotational velocity to this wall? no
Velocity Magnitude (m/s)          0
X-Component of Wall Translation    1
Y-Component of Wall Translation    0
Z-Component of Wall Translation    0
Define wall velocity components?   no
X-Component of Wall Translation (m/s) 0
Y-Component of Wall Translation (m/s) 0
Z-Component of Wall Translation (m/s) 0
Wall Roughness Height (m)         0
Wall Roughness Constant            0.5
Rotation Speed (rad/s)            0
X-Position of Rotation-Axis Origin (m) 0

```

Y-Position of Rotation-Axis Origin (m)	0
Z-Position of Rotation-Axis Origin (m)	0
X-Component of Rotation-Axis Direction	0
Y-Component of Rotation-Axis Direction	0
Z-Component of Rotation-Axis Direction	1
X-component of shear stress (pascal)	0
Y-component of shear stress (pascal)	0
Z-component of shear stress (pascal)	0
Specularity Coefficient	0

top

Condition	Value
Rotationally Periodic?	no

#### Solver Settings

##### Equations

Equation	Solved
Flow	yes
Modified Turbulent Viscosity	yes

##### Numerics

Numeric	Enabled
Absolute Velocity Formulation	yes

##### Relaxation

Variable	Relaxation Factor
Pressure	0.15000001
Density	1
Body Forces	1
Momentum	0.7
Modified Turbulent Viscosity	0.8
Turbulent Viscosity	1

##### Linear Solver

Variable	Solver Type	Termination Criterion	Residual Reduction Tolerance
Pressure	V-Cycle	0.1	
X-Momentum	Flexible	0.1	0.7
Y-Momentum	Flexible	0.1	0.7
Z-Momentum	Flexible	0.1	0.7
Modified Turbulent Viscosity	Flexible	0.1	0.7

##### Pressure-Velocity Coupling

Parameter	Value
Type	SIMPLE

##### Discretization Scheme

Variable	Scheme
Pressure	Standard
Momentum	Second Order Upwind
Modified Turbulent Viscosity	First Order Upwind

##### Solution Limits

Quantity	Limit
Minimum Absolute Pressure	1
Maximum Absolute Pressure	5e+10
Minimum Temperature	1

Maximum Temperature 5000  
Maximum Turb. Viscosity Ratio 100000